

Ultra-cool dwarfs: new discoveries, proper motions, and improved spectral typing from SDSS and 2MASS photometric colors

Z.H. Zhang^{1,3,2}, R. S. Pokorny¹, H. R. A. Jones², D. J. Pinfield², P.S. Chen¹, Z. Han¹,
D. Chen^{1,2}, M. C. Gálvez-Ortiz² and B. Burningham²

¹ National Astronomical Observatories/Yunnan Observatory, Chinese Academy of Sciences, Kunming 650011, China
e-mail: zenghuazhang@hotmail.com

² Centre for Astrophysics Research, Science and Technology Research Institute, University of Hertfordshire, College Lane, Hatfield AL10 9AB, U.K.
e-mail: h.r.a.jones@herts.ac.uk

³ Graduate School of Chinese Academy of Sciences, Beijing 100049, China

Received June 4, 2008; accepted January 14, 2009

ABSTRACT

Aims. We try to identify ultra-cool dwarfs from the seventh Data Release of the Sloan Digital Sky Survey (SDSS DR7) with SDSS i - z and r - z colors. We also obtain proper motion data from SDSS, 2MASS, and UKIDSS and improve spectral typing from SDSS and 2MASS photometric colors.

Methods. We selected ultra-cool dwarf candidates from the SDSS DR7 with new photometric selection criteria, which are based on a parameterization study of known L and T dwarfs. The objects are then cross-identified with the Two Micron All Sky Survey and the Fourth Data Release of the UKIRT Infrared Deep Sky Survey (UKIDSS DR4). We derive proper motion constraints by combining SDSS, 2MASS, and UKIDSS positional information. In this way we are able to assess, to some extent, the credence of our sample using a multi epoch approach, which complements spectroscopic confirmation. Some of the proper motions are affected by short baselines, but, as a general tool, this method offers great potential to confirm faint L dwarfs as UKIDSS coverage increases. In addition we derive updated color-spectral type relations for L and T dwarfs with SDSS and 2MASS magnitudes.

Results. We present 59 new nearby M and L dwarfs selected from the imaging catalog of the SDSS DR7, including proper motions and spectral types calculated from the updated color-spectral type relations, and obtain proper motions from SDSS, 2MASS, and UKIDSS for all of our objects.

Key words. star: low-mass, brown dwarfs

1. Introduction

Brown dwarfs occupy the mass range between the lowest mass stars and the highest mass planets. The central temperature of a brown dwarf is not high enough to achieve stable hydrogen burning like a star, but all brown dwarfs will undergo short periods of primordial deuterium burning very early in their evolution. Since the first discovery of an L dwarf (GD165 B; Becklin & Zuckerman 1988) and a T dwarf (Gl229 B; Nakajima et al. 1995), the projects searching for brown dwarfs have involved a number of large scale surveys, for example, the Deep Near-Infrared Survey (DENIS; Epchtein et al. 1997), the Two Micron All Sky Survey (2MASS; Skrutskie et al. 2006) and the Sloan Digital Sky Survey (SDSS; York et al. 2000; Adelman-MaCarthy et al. 2008). 554 L dwarfs and 145 T dwarfs have been found in large scale sky surveys in the last decade (by January 2009, see, DwarfsArchives.org for a full list). 31 of L or T dwarfs have been found in DENIS (e.g. Delfosse et al. 1997), 185 in SDSS (e.g. Fan et al. 2000; Geballe et al. 2002; Hawley et al. 2002; Schneider et al. 2002; Knapp et al. 2004; Chiu et al. 2006), and 368 in 2MASS (e.g. Burgasser et al. 1999, 2002, 2004; Kirkpatrick et al. 1999, 2000; Gizis et al. 2000; Cruz et al. 2003, 2007; Kendall et al. 2003, 2007;Looper et al. 2007).

More recently, the UKIRT Infrared Deep Sky Survey (UKIDSS; Lawrence et al. 2007) is beginning to be very effective in searching for T dwarfs (Kendall et al. 2007; Lodieu et al. 2007; Warren et al. 2007; Burningham et al. 2008; Pinfield et al. 2008).

In this paper we report the discovery of 59 late M and L dwarfs from the main photometric catalog of SDSS DR7.1. The photometric selection processes are presented in section 2. The red optical spectra of the 36 new late M and L dwarfs from SDSS are presented in section 3. Polynomial fitting for color-spectral type relationships are derived in section 4. The UKIDSS matches for 23 ultra-cool dwarf candidates without SDSS spectra are presented in section 5, and section 6 presents some further discussion.

2. Photometric selection

The Sloan Digital Sky Survey uses a dedicated 2.5 m telescope located at Apache Point Observatory (APO) in New Mexico. It is equipped with a large format mosaic CCD camera to image the sky in five optical bands (u , g , r , i , z), and two digital spectrographs to obtain the spectra of galaxies, quasars and late type stars selected from the imaging data (York et al. 2000). The SDSS DR7 imaging data covers about 8420 deg^2 of the main survey area (legacy sky), with information on roughly 230 million distinct photometric objects. The SDSS magnitude limits

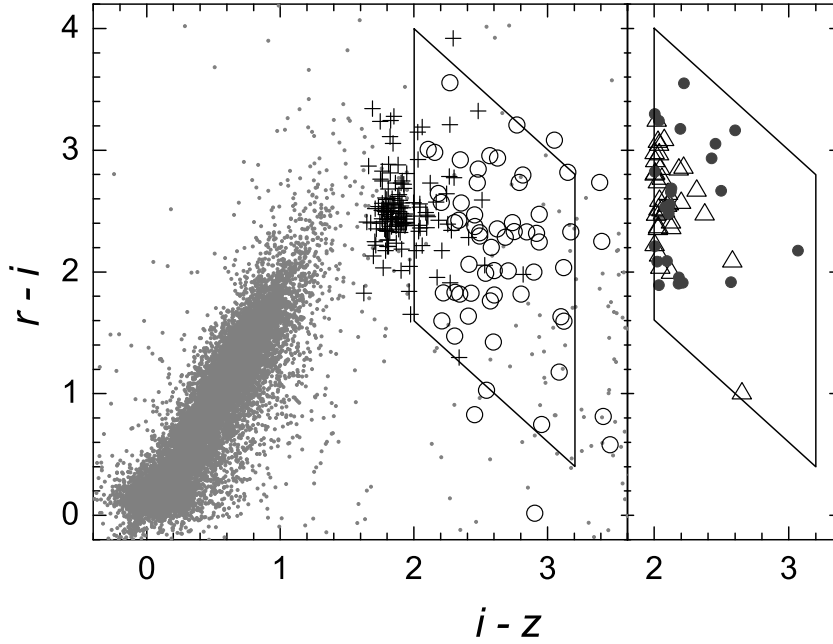


Fig. 1. $r - i$ vs. $i - z$ diagram for previously identified L dwarfs (left hand panel) and new M and L dwarfs (right hand panel). Previously identified L0-L4.5 and L5-L9.5 dwarfs are shown as *crosses* and *open circles* respectively. The 36 new M and L dwarfs with measured spectral types (from SDSS spectroscopy) are shown as *open triangles*, and the 23 new ultracool dwarf candidates (no SDSS spectra available) that we have cross-matched in UKIDSS DR4 are shown as *filled circles*. As a comparison, 24300 point sources with $15 < z < 20.5$ from 10 deg^2 of SDSS coverage are shown as *dots*. A parallelogram shows the boundary limits of our color selection.

(95% detection repeatability for point sources) for the u , g , r , i and z bands are 22.0, 22.2, 22.2, 21.3 and 20.5 respectively.

The $i - z$ color is particularly useful for L dwarf selection (as first pioneered by Fan et al. (2000), and expanded on by others e.g. via the i -band drop-out method; e.g. Chiu et al. 2006). For the cooler T_{eff} T dwarfs, almost all of the radiation is emitted beyond 10000 \AA , and as such these objects are optically much fainter than L dwarfs. SDSS is thus significantly less sensitive to T dwarfs than to L dwarfs, but has the sensitivity to identify L dwarfs out to distances well beyond 100pc.

We have made a study of L dwarf color-color parameter-space using previously identified L and T dwarfs with photometric data available from either SDSS or 2MASS (from DwarfsArchives.org, as of September 25, 2007). Where two spectral types are available (optical and infrared) we used the mean average type. A total of 431 L and 84 T dwarfs have 2MASS photometric data (J , H , K), and 193 L and 46 T dwarfs have SDSS photometric data (u , g , r , i , z). We excluded L and T dwarfs known to be unresolved binary systems from our study. These optical and near-infrared parameter spaces are shown in the left-hand panels of Figures 1 and 2, where crosses indicate early L dwarfs (L0-L4.5) and open circles indicate mid-late L dwarfs (L5-L9.5). Using these plots we have identified regions of color space that contain the vast majority of mid-late L dwarfs. We chose $i - z > 2$ to avoid too much contamination from red dwarfs, although this does leads to missing many early L dwarfs. Figure 1 shows the selection cuts in the $r - i$ versus

$i - z$ diagram, in which a parallelogram shows the boundary limits. Two two sloping lines show the boundary limits $r - z = 3.6$ and $r - z = 6$, and the two vertical lines show $i - z = 2$ and $i - z = 3.2$. Taking into account also the photometric sensitivities of SDSS, we thus define a set of SDSS mid-late L dwarf photometric selection criteria as follows:

$$19 < i < 23 \quad (1)$$

$$17 < z < 20 \quad (2)$$

$$3.6 < r - z < 6 \quad (3)$$

$$2 < i - z < 3.2 \quad (4)$$

Criterion (3) can also be written as

$$3.6 - (i - z) < r - i < 6 - (i - z) \quad (5)$$

in $r i z$ color-color space.

The left-hand panel of Figure 2 shows the $J - H$ vs. $H - K$ diagram for known L dwarfs. As for Figure 1 we define a set of color criteria to contain the majority of these L dwarfs. It is clear from Figure 2 that the L dwarfs appear reasonably well separated from the M dwarfs in this 2-color space (see also Burgasser et al. 2002), and we would thus expect to improve our sample refinement significantly by combining our optical selection with additional near infrared photometry. Our chosen 2MASS color selection criteria are shown in the Figure with solid lines, and are defined as:

$$J - H > 0.5 \quad (6)$$

$$H - K > 0.2 \quad (7)$$

$$J - K > 1 \quad (8)$$

More than 6000 candidates survived our color and magnitude optical selection from the main photometric catalog of SDSS DR7. Those candidates were matched with point sources in the 2MASS catalog (Skrutskie et al. 2006). We used a matching radius of $6''$ to ensure that any ultra-cool dwarfs with high proper motion could be matched, despite possible motion over a period of up to ~ 8 yrs (between epochs). A total of 700 SDSS objects were cross-matched in 2MASS. Because the imaging depth of SDSS is deeper than that of 2MASS, many of the fainter SDSS candidates could not be found in 2MASS. Thus some of the candidates get wrongly matched with their nearest brighter neighbors in 2MASS. These are removed by checking their images in both the SDSS and 2MASS databases. On closer inspection, 2MASS mis-matches are usually very apparent, since the mis-matching objects generally have their own SDSS counterpart that immediately rules them out as high proper motion. As a more subtle check of the cross-matching, we assessed the spectral energy distribution of candidates (estimated from their SDSS and 2MASS photometry), and identified candidates that appeared to have unusual SEDs when compared to those of known ultra-cool dwarfs. It was assumed that these objects were also 2MASS mis-matches, and they were removed from our selection. Tens of wrongly matched objects were thus identified and removed from our selection. Implementation of our near infrared color selection criteria (for candidates that did not have SDSS spectroscopy) allowed us to remove more than 300 objects from our sample via the $J - H$ and $H - K$ color cuts listed in equations 6, 7 and 8.

3. Red optical spectra from the SDSS

The SDSS imaging data are used to select in a uniform way different classes of objects whose spectra will be taken with the SDSS 2.5 m telescope (York et al. 2000). The target selection algorithms for spectroscopic follow up are described by Stoughton et al. (2002). The DR7.1 main spectroscopic data base includes data for around 1.2 million objects, and covers 7470 deg^2 . The wavelength coverage is from 3800 to 9200 Å with resolution $\lambda/(\Delta\lambda) = 1800$. The signal-to-noise ratio is better than 4 pixel^{-1} at $g = 20.2$ (Adelman-McCarthy et al. 2007). The spectra distributed by the SDSS have been sky subtracted and corrected for telluric absorption. The spectroscopic data are automatically reduced by the SDSS pipeline software.

Our final selection consisted of 275 objects of which 87 were cross-referenced with, and confirmed to be mostly L dwarfs. So 188 of these objects are new discoveries. Of these, 36 are confirmed through SDSS optical spectra. At first we only found 28 objects with SDSS spectra when we searched for the photometrically selected candidates in the SDSS spectroscopic catalog. Then we searched the spectra of SDSS color selected candidates with SDSS spectra which were removed with 2MASS criteria (6, 7, 8). We found six objects with SDSS spectra, three M9, one L0 and two L1 dwarfs. In Figure 2, we can see that the 2MASS criteria (6, 7, 8) are set for L dwarfs and some late M early L dwarfs will be missed, including these six objects. Another two objects were found with SDSS spectra which are faint and therefore missed by the 2MASS survey. Table 1 lists the SDSS names, SDSS r , i , z , 2MASS J , H , K and SDSS spectral types for these 36 spectroscopically confirmed ultracool dwarfs. Note that we also performed a cross-match with UKIDSS DR4 (see Section 5)

and that 23 objects without SDSS spectroscopy that were measured in UKIDSS are listed in Table 2. All remaining candidates (i.e. without SDSS spectroscopy or UKIDSS DR4 coverage) are given in Table 7 (online data).

In addition to the photometric and spectral type analysis we also derived proper motion constraints for our new sample, using the dual epoch coordinates from the SDSS and 2MASS databases and dividing any movement between the epochs by the observational epoch difference. Standard errors on these proper motions are calculated using the major axes of the position error ellipses from SDSS and 2MASS, and are dominated by the 2MASS positional uncertainties. Systematic astrometry errors between 2MASS-SDSS which have a shorter baseline, could lead to significant errors in calculating proper motions with coordinates and epoch differences, and can not be ignored. To correct the systematic offset of 2MASS-SDSS, we measured average proper motion of reference objects around every targets for which proper motion has been measured. Then we subtracted this average proper motion from the measured proper motion of each corresponding target. The number of reference objects ranged from around 100 to a few hundreds for different targets, with reference objects being selected to have low coordinate errors (mostly $<0.1''$, $<0.2''$ for the candidates with fewer reference objects). Reference objects are within $12'$, $15'$ or $20'$ of our targets depends on availability. These proper motions are also given in Tables 1 and 3 and 7 (Online Data). Their quality and accuracy is assessed in Section 5 through comparison with additional epoch image data and measurement of motion relative to nearby sources surrounding each ultracool dwarf (see also columns 10 and 11 in Table 1).

For the 11 M9 and 25 L dwarfs with SDSS spectra. We assigned their spectral types by comparison with the SDSS spectral sequence of previously found M, L and T dwarfs as shown in Figure 3, the dwarf classification scheme of Kirkpatrick et al. (1999), SDSS spectra of M and L dwarfs published by Hawley et al. (2002) and the low-mass dwarf template spectra from SDSS (Bochanski et al. 2007). One of the major points we have considered in the comparison is the shape of the normalized spectrum, such as the width of KI region around 7700 Å and the relative flux in the region from 8400 Å to 9000 Å. Another major point is the slope of the spectrum in the band from 8700 Å to 9200 Å. The last criterion is the depth of absorption lines which can be recognized in some spectra, such as NaI $\lambda\lambda 8183, 8195$, CrH $\lambda 8661$, FeH $\lambda 8692$ and CsI $\lambda\lambda 8521, 8944$. NaI $\lambda\lambda 8183, 8195$ is a major feature of late M dwarfs. CrH $\lambda 8661$ is equal in strength to FeH $\lambda 8692$ for L4 dwarfs, and stronger for L5 dwarfs. CsI keeps strengthening from L1 to L8 type (Kirkpatrick et al. 1999). Finally, to double check the spectral type of each spectrum, we subtract the spectrum of a ultra-cool dwarf which has the same spectral type and has a good quality, and find a good agreement within our errors.

We note that our selected objects can not be giants because of the presence of the high gravity features such as KI, NaI and FeH, which are characteristic of dwarfs (e.g., Bessell 1991). Figure 3 shows 8 spectra of previously found M, L and T dwarfs as a comparison. SDSS J1428+5923 was recently confirmed and spectral-typed using its infrared spectrum as an L5 dwarf using the Two Micron Proper Motion (2MUPM) survey, under the name 2MASS J14283132+5923354 (Schmidt et al. 2007). SDSS J0249-0034, SDSS J1048+0111, SDSS J1653+6231 and SDSS J1331-0116 were classified by Hawley et al. (2002). SDSS J1221+0257 and SDSS J1051+5613 were discovered by

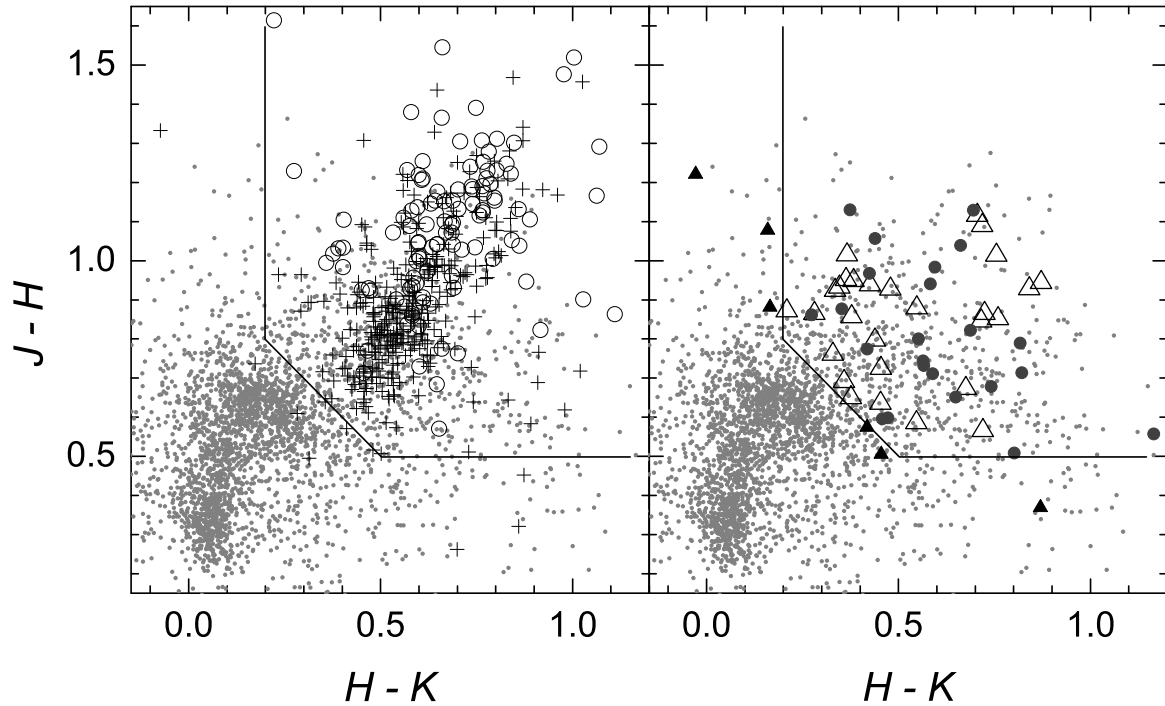


Fig. 2. $J - H$ vs. $H - K$ diagram for previously identified L dwarfs (left hand panel) and new M and L dwarfs (right hand panel). Symbols are as in Figure 1 except that six of the new spectroscopically confirmed dwarfs (three M9, one L0 and two L1) are indicated with filled triangles, because they lie outside our 2MASS photometric selection criteria (solid lines). Note that the 2MASS criteria are only applied when selecting photometric candidates, and not when SDSS spectra are available. For comparison, the plot shows 2800 sources (dots) taken from 3.14 deg^2 of 2MASS sky.

Reid et al. (2008), and SDSS J0330–0025 was discovered by Fan et al. (2000).

Figures 4 and 5 shows the SDSS spectra of the 36 M and L dwarfs found in this work. The spectra shortward of 6000 \AA are flat and noisy, and are not shown. The spectral types of our candidates extend from M9 to L6, and the spectral typing errors are estimated as about $\pm 1 \sim 2$ sub-type. These SDSS spectra have been smoothed by 11 pixels and have been normalized to one at 8250 \AA . There is a straight line in the spectrum of SDSS J1036+3724 which is an artifact. There is another artificial straight line in the spectrum of SDSS J1431+1436 across 8400 \AA . The spectra of SDSS J0903+0114, SDSS J1329+5317, SDSS J1410+1329 and SDSS J1720+6155 are noisy which made it more difficult to assign their spectral types.

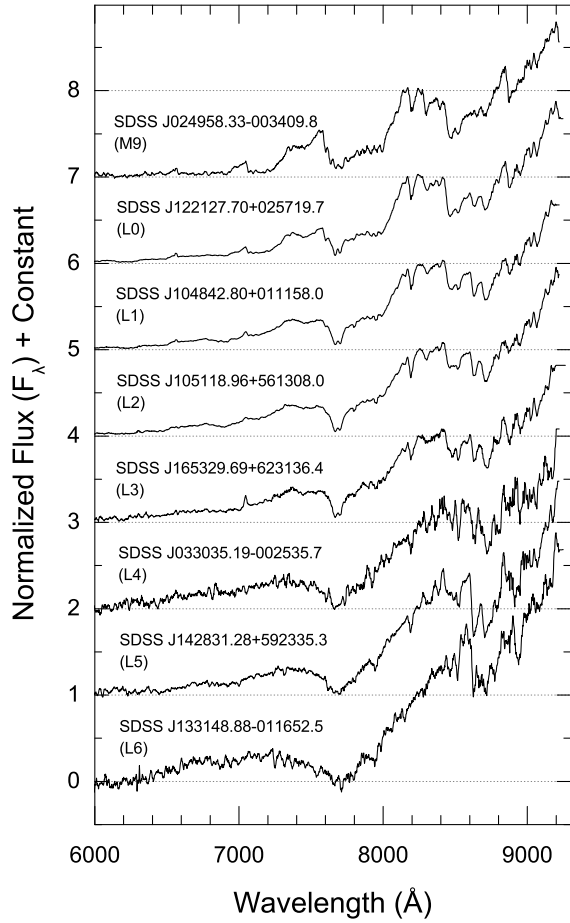


Fig. 3. SDSS spectra of 8 previously found M and L dwarfs, used for spectral typing. All spectra have been normalized to one at 8250 \AA and vertically offset for clarity.

Table 1. SDSS and 2MASS photometry of objects with SDSS spectra.

SDSS Name	SDSS r	SDSS i	SDSS z	2MASS J	2MASS H	2MASS K	P. M. ^a ("yr ⁻¹)	P. M. ^b Angle	P. M. ^c ("yr ⁻¹)	P. M. ^c Angle	Spe. Type	S.T.by ^d Colors
SDSS J010718.70+132656.1 ^e	23.24±0.31	20.74±0.06	18.68±0.04	16.58±0.15	16.21±0.19	15.34 ...	0.51±0.13	289±15	0.43 ...	107 ...	M9	...
SDSS J012052.58+151827.3	23.54±0.58	20.69±0.08	18.65±0.04	16.39±0.13	15.44±0.10	14.57±0.12	0.48±0.09	116±11	0.13±0.09	209±32	M9	...
SDSS J075256.70+173433.8	23.91±0.53	20.94±0.06	18.93±0.04	16.43±0.12	15.80±0.17	15.34 ...	0.13±0.04	226±16	0.06±0.06	139±136	L0	L1
SDSS J080322.77+123845.3	23.09±0.22	20.73±0.05	18.60±0.03	16.31±0.08	15.44±0.08	15.23±0.11	0.13±0.03	223±12	0.28±0.23	199± 3	L2.5	L1
SDSS J084016.42+543002.1 ^e	23.05±0.31	20.83±0.06	18.83±0.05	16.39±0.12	15.51±0.13	15.35±0.15	0.51±0.81 ^f	280 ...	1.66±1.56 ^f	298±61	L1	L1.5
SDSS J084751.48+013811.0	23.96±0.71	20.89±0.08	18.86±0.06	16.23±0.13	15.12±0.10	14.41±0.09	0.66±0.47 ^f	263 ...	1.05±1.39 ^f	262±39	L4	L3.5
SDSS J090023.68+253934.3	23.55±0.40	21.47±0.09	18.89±0.04	16.43±0.12	15.41±0.12	14.66±0.08	0.04±0.03	154±49	0.05±0.05	165±12	L6	L4.5
SDSS J090320.92+504050.6	23.46±0.42	20.55±0.05	18.54±0.03	16.42±0.12	15.49±0.13	15.15±0.14	0.17±0.17	301±73	0.24±0.19	192±113	M9	...
SDSS J090347.55+011446.0	23.47±0.45	21.07±0.08	18.94±0.05	16.45±0.14	15.60±0.11	14.89±0.13	0.67±0.71 ^f	205 ...	1.54±1.43 ^f	252±71	L2	L2.5
SDSS J091714.76+314824.8	23.20±0.24	20.85±0.04	18.82±0.03	16.30±0.10	15.73±0.14	15.01±0.13	0.02±0.04	145 ...	0.03±0.02	196±73	L2	L.5
SDSS J100016.92+321829.4	23.71±0.54	21.04±0.11	18.73±0.05	16.62±0.12	15.70±0.11	15.36±0.17	0.44±0.05	243± 6	0.45±0.40	245± 3	L3.5	L1.5
SDSS J100435.88+565757.4	23.63±0.49	20.79±0.07	18.61±0.04	16.67±0.11	15.81±0.10	15.43±0.17	0.19±0.12	286±38	... ^g	...	M9	...
SDSS J100817.07+052312.9 ^e	23.79±0.46	21.02±0.06	18.97±0.04	16.76±0.16	16.19±0.19	15.77±0.28	0.07±0.18	106 ...	0.30±0.30	142± 5	M9	...
SDSS J102316.59+011549.6	23.20±0.41	21.07±0.09	19.03±0.05	16.76±0.16	15.91±0.18	15.15±0.17	0.28±0.28	272 ...	1.50±1.23	227±98	M9	...
SDSS J102356.38+242430.3	22.59±0.17	21.59±0.12	18.94±0.05	M9	...
SDSS J102947.68+483412.2	23.68±0.49	20.89±0.07	18.88±0.05	16.76±0.19	16.04±0.21	15.59±0.24	0.45±0.18	237±24	0.23±0.16	112±82	L0	L2
SDSS J103602.44+372448.5	22.75±0.19	20.76±0.06	18.63±0.04	16.42±0.12	15.54±0.13	14.99±0.11	0.10±0.03	176±17	0.12±0.11	153±48	L0	L1
SDSS J104407.47+015742.0	23.23±0.32	20.87±0.07	18.84±0.05	16.59±0.16	15.65±0.13	15.22±0.20	2.51±1.22	113±29	1.46±1.08	168±65	L1	L0.5
SDSS J104922.45+012559.2	23.85±0.59	21.00±0.09	18.78±0.04	15.88±0.07	14.95±0.07	14.11±0.06	0.07±0.14	21 ...	0.13±0.16	200±23	L5	L5
SDSS J110009.62+495746.5	22.57±0.19	20.08±0.03	18.00±0.02	15.28±0.04	14.19±0.04	13.47±0.03	0.25±0.03	241± 8	0.23±0.20	230±13	L4	L4
SDSS J112242.26+364928.6	23.29±0.31	20.75±0.05	18.65±0.04	16.54±0.11	15.61±0.11	15.13±0.11	0.07±0.03	106±27	0.04±0.03	154±84	M9	...
SDSS J114201.95+521917.0 ^e	21.71±0.08	19.13±0.02	17.09±0.01	15.08±0.05	14.57±0.07	14.12±0.05	0.20±0.05	219±13	... ^g	...	M9	...
SDSS J115013.17+052012.3	23.75±0.39	21.28±0.07	18.91±0.04	16.25±0.14	15.46±0.14	15.02±0.17	0.72±0.24	260±20	... ^g	...	L5.5	L3
SDSS J132926.03+531733.9 ^e	23.84±0.50	20.87±0.06	18.84±0.04	16.82±0.20	15.59±0.17	15.62±0.24	0.19±0.12	177±40	0.05±0.05	152±83	L1	L1
SDSS J133257.73+325813.1 ^e	23.20±0.25	20.73±0.04	18.72±0.03	16.57±0.11	15.49±0.11	15.33±0.12	0.15±0.04	224±15	0.12±0.12	218±32	L0	L0.5
SDSS J134025.14+524505.0	23.71±0.55	21.14±0.08	18.94±0.04	16.69±0.15	15.67±0.14	15.31±0.12	0.21±0.11	75±33	0.15±0.16	159±81	M9	...
SDSS J141011.14+132900.8	24.11±0.49	21.03±0.07	18.96±0.05	16.85±0.14	15.89±0.15	15.53±0.19	0.18±0.06	279±21	0.17±0.11	276± 5	L4	...
SDSS J143130.77+143653.4	22.25±0.12	19.69±0.02	17.58±0.02	15.15±0.04	14.50±0.05	14.13±0.06	0.45±0.02	259± 3	0.45±0.37	261± 3	L2	L1.5
SDSS J143832.63+572216.9	23.45±0.40	20.81±0.06	18.71±0.04	15.96±0.07	15.10±0.08	14.37±0.06	0.20±0.05	86±13	0.12±0.14	75±43	L5	L3.5
SDSS J151136.24+353511.4	23.45±0.35	20.72±0.05	18.69±0.03	16.29±0.10	15.62±0.11	14.95±0.12	0.06±0.04	179±48	0.16±0.13	133±70	L1	L1
SDSS J154502.87+061807.8	23.91±0.42	20.87±0.05	18.83±0.04	16.37±0.11	15.60±0.12	15.28±0.16	0.21±0.08	282±23	0.20±0.14	263±31	L4	L1
SDSS J154628.38+253634.3	22.66±0.14	20.15±0.03	18.12±0.02	15.76±0.07	15.07±0.08	14.71±0.08	0.51±0.03	286± 4	0.34±0.30	283±13	L1	L0.5
SDSS J155215.38+065041.5	24.23±0.53	20.99±0.06	18.97±0.04	16.78±0.15	15.91±0.14	15.63±0.21	0.01±0.09	264 ...	0.18±0.18	294±11	L0	L0.5
SDSS J161840.27+202045.6	23.40±0.26	20.60±0.04	18.59±0.03	16.15±0.09	15.20±0.07	14.81±0.09	0.15±0.04	35±14	0.04±0.04	205±97	M9	...
SDSS J172006.69+615537.7	23.35±0.52	21.32±0.13	19.27±0.08	L3	...
SDSS J211846.77-001044.6	23.28±0.30	20.80±0.06	18.73±0.04	16.20±0.11	15.62±0.16	15.07±0.13	0.16±0.19	18 ...	0.29±0.27	223±103	L1	L1

Note: SDSS magnitude limits (95% detection repeatability for point sources) for r , i and z bands are 22.2, 21.3 and 20.5 respectively.

^a 2MASS-SDSS data-base proper motions - found by dividing the difference between the 2MASS and SDSS coordinates (from the respective databases) by the observational epoch difference. Standard errors are calculated using the major axes of the position error ellipses from 2MASS and SDSS.

^b Error ellipses of 2MASS and SDSS overlap for some objects, for which position angle errors are not meaningful.

^c 2MASS-SDSS relative proper motions - found by specifically measuring the relative movement of the ultracool dwarfs with respect to nearby reference objects in the 2MASS and SDSS images.

^d Spectral types are based on the relationship between spectral type and SDSS and 2MASS colors ($i-z$, $i-J$, $i-H$, $i-K$ are used largely and $r-i$, $z-J$, $z-H$, $z-K$ with less weight).

^e Objects with SDSS spectra which do not accord with the 2MASS color criteria (6, 7, 8).

^f Objects only have a baseline of ~ 3 months.

^g We do not measure their proper motions for they are very faint in 2MASS images or only have a few nearby reference objects.

Table 2. Photometric data of UKIDSS matched L dwarf candidates

SDSS Name	SDSS r	SDSS i	SDSS z	2MASS J	2MASS H	2MASS K	UKIDSS Y	UKIDSS J	UKIDSS H	UKIDSS K	Sp.Type ^a
J004759.59+135332.0 ^b	24.78±0.88	22.11±0.28	19.61±0.10	16.81±0.16	16.10±0.17	15.51±0.19	18.03±0.03	17.22±0.03	16.52±0.03	16.00±0.03	L3.5
J015141.04-005156.5 ^c	22.23±0.15	19.70±0.03	17.61±0.02	15.10±0.05	14.27±0.04	13.59±0.05	16.24±0.01	15.02±0.00	14.29±0.00	13.65±0.00	L2
J022927.95-005328.5	24.19±0.64	21.54±0.11	19.41±0.07	16.49±0.10	15.75±0.10	15.18±0.14	...	16.62±0.02	15.82±0.02	15.15±0.02	L3.5
J073241.77+264558.9	24.31±0.46	22.40±0.18	19.83±0.08	17.37±0.21	16.81±0.25	15.64±0.19	...	17.55±0.02	L4.5
J074436.02+251330.5	24.28±0.49	21.23±0.07	18.77±0.03	17.17±0.25	16.04±0.21	15.66±0.22	...	16.68±0.01	L1
J075754.16+221604.9	23.34±0.36	21.45±0.10	19.41±0.06	16.61±0.13	16.10±0.22	15.30±0.14	...	16.87±0.01	L2.5
J081303.96+243355.9	23.41±0.38	21.32±0.08	19.30±0.05	16.67±0.12	15.63±0.12	14.97±0.09	...	16.57±0.01	L3
J081409.45+260250.4	25.06±0.67	21.88±0.15	19.69±0.10	17.18±0.18	16.50±0.21	15.76±0.19	...	17.25±0.02	L2
J083613.45+022106.2 ^c	22.36±0.16	19.12±0.02	17.09±0.01	14.76±0.04	14.17±0.04	13.71±0.04	15.73±0.01	14.72±0.00	14.18±0.00	13.68±0.00	L0.5
J092745.81+010640.4	24.03±0.68	21.34±0.10	19.21±0.06	16.97±0.20	16.18±0.21	15.37±0.21	18.05±0.03	17.11±0.01	16.55±0.02	15.99±0.03	L1
J094624.37+344639.8	23.40±0.30	20.92±0.05	18.82±0.03	16.44±0.10	15.79±0.13	15.14±0.12	...	16.33±0.01	L1
J095941.47+114146.0	23.51±0.38	21.30±0.08	19.29±0.05	16.43±0.14	15.66±0.13	15.24±0.19	15.27±0.01	L3
J121238.73+000721.6	24.02±0.66	20.85±0.09	18.25±0.03	15.81±0.10	15.01±0.09	14.46±0.09	...	15.69±0.01	L3.5
J133131.70+122531.4	24.62±0.66	21.32±0.10	19.32±0.05	16.78±0.16	15.72±0.17	15.28±0.15	17.83±0.03	16.72±0.01	16.03±0.02	15.46±0.01	L2.5
J134531.43+001551.2	24.14±0.51	21.59±0.11	19.47±0.08	16.94±0.21	15.98±0.14	15.55±0.23	18.19±0.03	16.95±0.02	16.19±0.02	15.60±0.02	L2.5
J150153.00-013507.1	22.71±0.25	20.80±0.07	18.62±0.05	16.08±0.09	14.95±0.07	14.26±0.09	15.02±0.01	14.25±0.01	L3.5
J154236.26-004545.9	24.71±0.79	21.78±0.15	19.35±0.06	16.71±0.13	15.98±0.14	15.41±0.20	18.07±0.02	16.83±0.02	16.21±0.02	15.64±0.02	L3.5
J154432.77+265551.2	23.22±0.23	21.31±0.07	19.10±0.04	16.22±0.10	15.24±0.10	14.64±0.10	...	16.23±0.01	L4.5
J154740.16+053208.3	23.39±0.30	20.57±0.04	18.57±0.03	16.18±0.10	15.58±0.11	15.11±0.16	17.25±0.01	16.18±0.01	15.58±0.01	15.02±0.01	L0.5
J161711.68+322249.5	24.80±0.88	21.25±0.12	19.03±0.06	16.56±0.13	15.69±0.15	15.42±0.16	...	16.68±0.01	L2
J232715.71+151730.4	23.26±0.28	21.31±0.09	19.13±0.05	16.29±0.11	15.35±0.09	14.77±0.13	17.54±0.02	16.20±0.01	15.36±0.01	14.68±0.01	L5
J234040.33-003337.2	23.54±0.35	21.45±0.10	19.35±0.06	17.06±0.16	16.34±0.23	15.52±0.20	17.94±0.03	17.03±0.02	16.46±0.02	16.01±0.04	L1
J234513.85+002441.6	24.80±0.71	22.63±0.29	19.56±0.08	16.78±0.16	15.90±0.20	15.55±0.19	17.67±0.03	...	16.21±0.02	15.59±0.02	L8.5

Notes: UKIDSS magnitude limits for Y , J , H and K bands are 20.5, 20.0, 18.8 and 18.4 respectively. All magnitudes here are Vega based. We use 0.1'' as a typical position error for UKIDSS. Error ellipses of 2MASS and SDSS overlap for some objects for which proper motion angle errors are not listed.

^a Spectral types are based on the relationship between spectral type and SDSS and 2MASS colors ($i-z$, $i-J$, $i-H$, $i-K$ are used largely and $r-i$, $z-J$, $z-H$, $z-K$ with less weight).

^b It is merged with a nearby faint galaxy in 2MASS image, so its 2MASS photometric data is not reliable. The spectral type is based on SDSS-UKIDSS colors ($i-J$, $i-H$ and $i-K$) according to equation (9).

^c Data errors of J , H , K bands are less than 0.005.

Using the relationship between absolute J and z band magnitudes and spectral types (Hawley et al. 2002), we estimated the approximate distance of the 36 new M and L dwarfs. Generally, early and mid L dwarfs in our sample are between 25 and 100 pc, and the M dwarfs beyond 100 pc.

4. Color-spectral type relationships

To estimate the spectral types of our ultra-cool dwarf candidates without spectra, we need to know the relationships between spectral types and colors. Hawley et al. (2002) gave the correlation between spectral type and average color for each subtype range from M0 to T6. The relationship is good for M dwarfs, but has large errors for L and T dwarfs. With a much larger number of L and T dwarfs now available, we made a study of the relationships between spectral types of L and T dwarfs and their colors from SDSS and 2MASS. To construct these relationships we used the same data set as that for the photometric selection criteria (see section 2). SDSS colors $r-i$, $i-z$, 2MASS colors $J-H$, $H-K$ and optical-near infrared colors $i-J$, $i-H$, $i-K$, $z-J$, $z-H$, $z-K$ are involved. We fit these relationships with a united polynomial equation,

$$color = a + b(type) + c(type)^2 \quad (9)$$

where type is a number designed to encompass the full range of M, L and T spectral classes (type=10 for L0, 15 for L5, 20 for T0, 25 for T5). Polynomial parameters a , b and c are different for different color ranges and our range of calculated values can be found in Table 4. As well as spectral type ranges, correlation coefficient R and sensitivity indices for the fitting equations are also available in Table 4, where the sensitivity index is defined as the rate of change of color with spectral type, and is thus an indication of the usefulness of a color as a spectral type estimator. Calculated values of the various colors are presented in Table 5 for spectral sub-types between L0 and T7.5. The $i-z$, $i-J$, $i-H$ and $i-K$ colors are the most sensitive to spectral type, and the first three of these are plotted as a function of spectral type in Figure 6.

5. Cross matching the new sample with UKIDSS

To provide an additional epoch of deeper near infrared measurements that could improve candidate characterization (particularly for candidates without SDSS spectroscopy), we cross-matched our SDSS DR7 candidates with the Fourth Data Release of the UKIDSS Large Area Survey (Lawrence et al. 2007). UKIDSS magnitude limits for the Y , J , H and K bands are 20.5, 20.0, 18.8 and 18.4 respectively. We found that 23 of our candidates (without SDSS spectra) and 7 of our spectroscopically confirmed objects have UKIDSS DR4 counterparts. Table 2 lists the SDSS names, r , i , z , 2MASS J , H , K , UKIDSS Y , J , H , K and color-estimated spectral types (see Section 4) for the objects without spectroscopy, and Table 3 presents the additional UKIDSS information for 7 of the spectroscopic objects from Table 1.

Figure 7 shows the $Y-J$ versus $J-H$ diagram for the 15 candidates that had UKIDSS Y detections. In general these all had UKIDSS YJH magnitudes but in 2 cases we had to transform a 2MASS J into a UKIDSS J following the conversion of Hewett et al. 2006. This 2-color diagram can provide additional information on ultra-cool dwarf spectral types (e.g. Hewett et al. 2006). For example, the SDSS/2MASS colors of SDSS J2345-0024 suggest a spectral type between L7 and T2. However, Figure 7

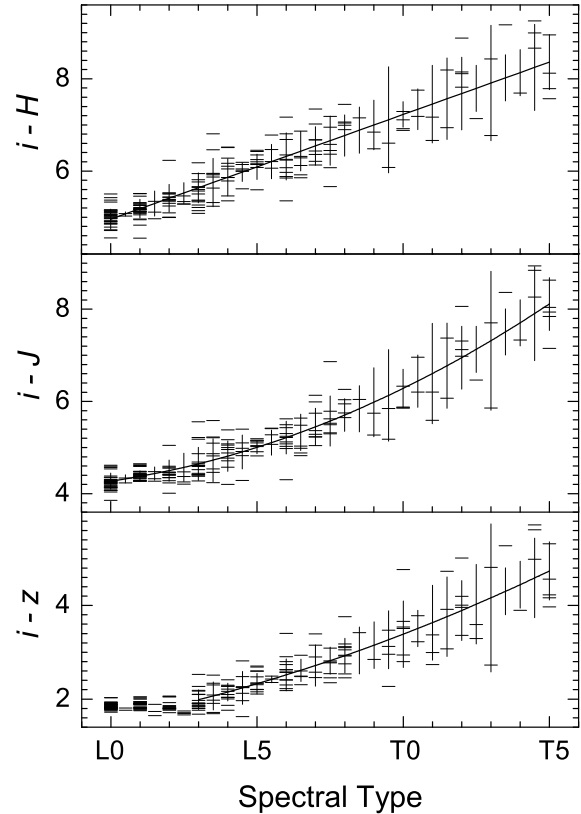


Fig. 6. Polynomial fitting for color-spectral type relationships are indicated with a solid line. The error bars of fitted colors indicate the standard deviation at each subtype. We used 0.5 as the error, if there is only one object available for a given subtype.

suggests that SDSS J2345-0024 is more likely an early T dwarf than a late L dwarf.

To further assess the proper motions that we derive for all candidates using the coordinate and epoch information stored in the SDSS and 2MASS databases, we have measured additional proper motion constraints using several combinations of multi-epoch data (SDSS/UKIDSS, 2MASS/UKIDSS and 2MASS/SDSS combinations), as well as by measuring the motion of our ultracool dwarf candidates with respect to reference objects within $6'$ in the SDSS z and UKIDSS Y , J , H and K images. For the relative proper motions, we used the Iraf routines GEOMAP and GEOXYTRAN to transform the pixel coordinates from the SDSS images into the pixel coordinate system of the UKIDSS images. Visual inspection of the image data revealed a small number of problematic sources. SDSS J0047+1353 is merged with a very nearby galaxy in the 2MASS image. In the main however, four separate proper motion measurements were made (combining z/Y , z/J , z/H and z/K) where possible, and an average proper motion taken. UKIDSS centroiding accuracy was estimated from the standard deviation of these four measurements, and we also factored in a centroiding uncertainty associated with the SDSS z -band epoch, which we estimated to be $0.1''$ (1/4 of an SDSS pixel) for these faint sources. The relative proper motions measured from 2MASS and SDSS images are given in columns 10 and 11 of Table 1 (for the spectroscopically confirmed objects). The relative

Table 3. Seven objects with SDSS spectra matched in UKIDSS

SDSS Name	UKIDSS <i>Y</i>	UKIDSS <i>J</i>	UKIDSS <i>H</i>	UKIDSS <i>K</i>	Proper Motion ^a ("yr ⁻¹)	Proper Motion Angle ^b
SDSS J012052.58+151827.3	17.11±0.02	16.09±0.01	15.50±0.01	14.92±0.01	0.04±0.02	105±36
SDSS J084751.48+013811.0	17.38±0.02	16.09±0.01	15.22±0.01	14.45±0.01	0.03±0.02	242 ...
SDSS J090347.55+011446.0	17.58±0.02	...	15.59±0.01	14.96±0.01	0.03±0.02	259 ...
SDSS J091714.76+314824.8	...	16.36±0.01	0.03±0.03	345 ...
SDSS J100817.07+052312.9	16.36±0.02	15.89±0.03	0.21±0.03	139±10
SDSS J154502.87+061807.8	17.35±0.02	16.21±0.01	15.62±0.01	15.07±0.01	0.14±0.04	251±25
SDSS J155215.38+065041.5	15.93±0.01	15.32±0.01	0.02±0.04	356 ...

^a SDSS-UKIDSS data-base proper motions - found by dividing the difference between the SDSS and UKIDSS coordinates (from the respective databases) by the observational epoch difference. Standard errors are calculated using the major axes of the position error ellipses from SDSS and UKIDSS.

^b Error ellipses of SDSS and UKIDSS overlap for some objects for which position angle errors are not meaningful.

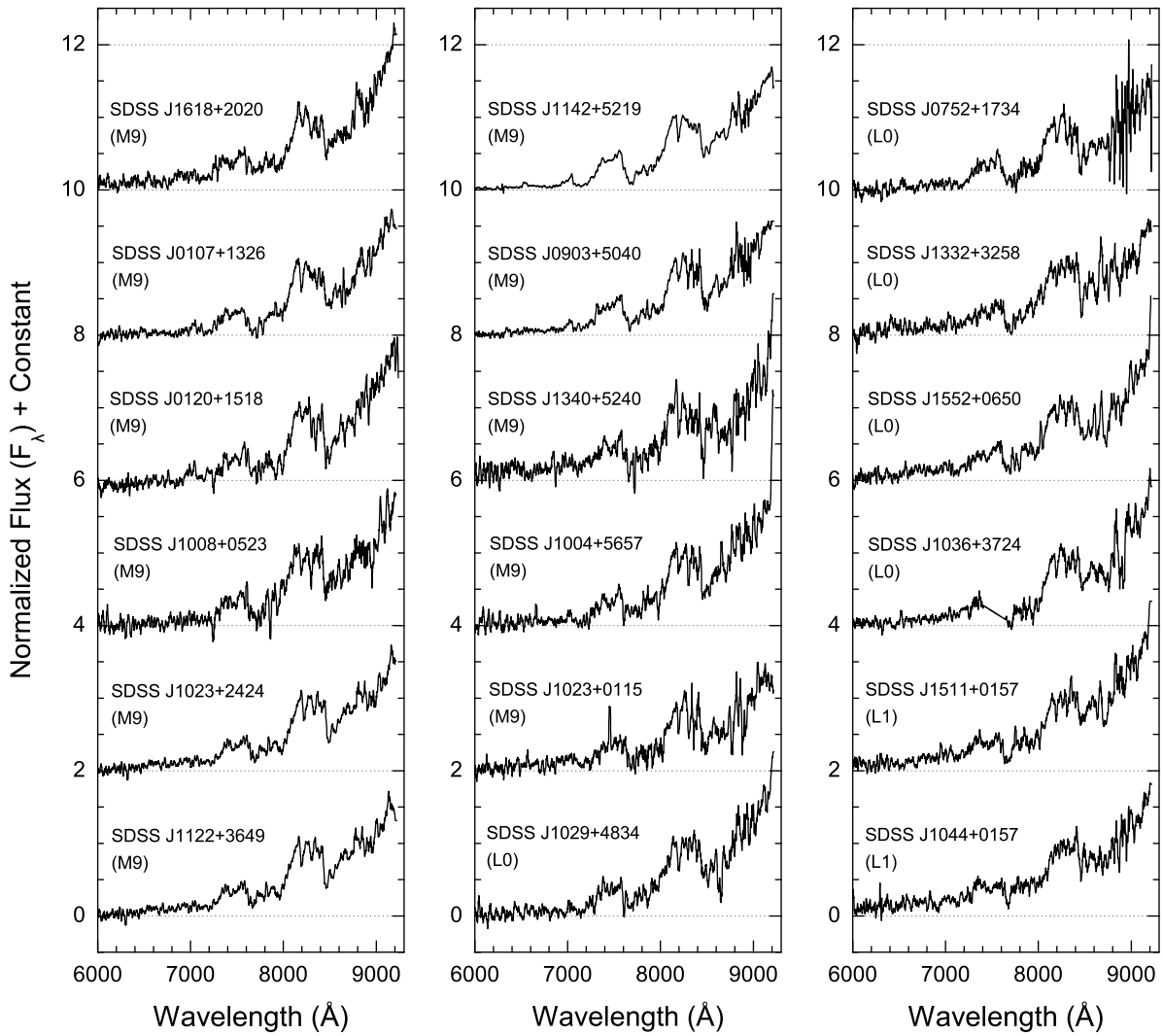


Fig. 4. The SDSS spectra of new M and L dwarfs. Spectral types are given in brackets. The spectra are normalized to one at 8250 Å and offset from one another for clarity. All the spectra are taken from the SDSS archive.

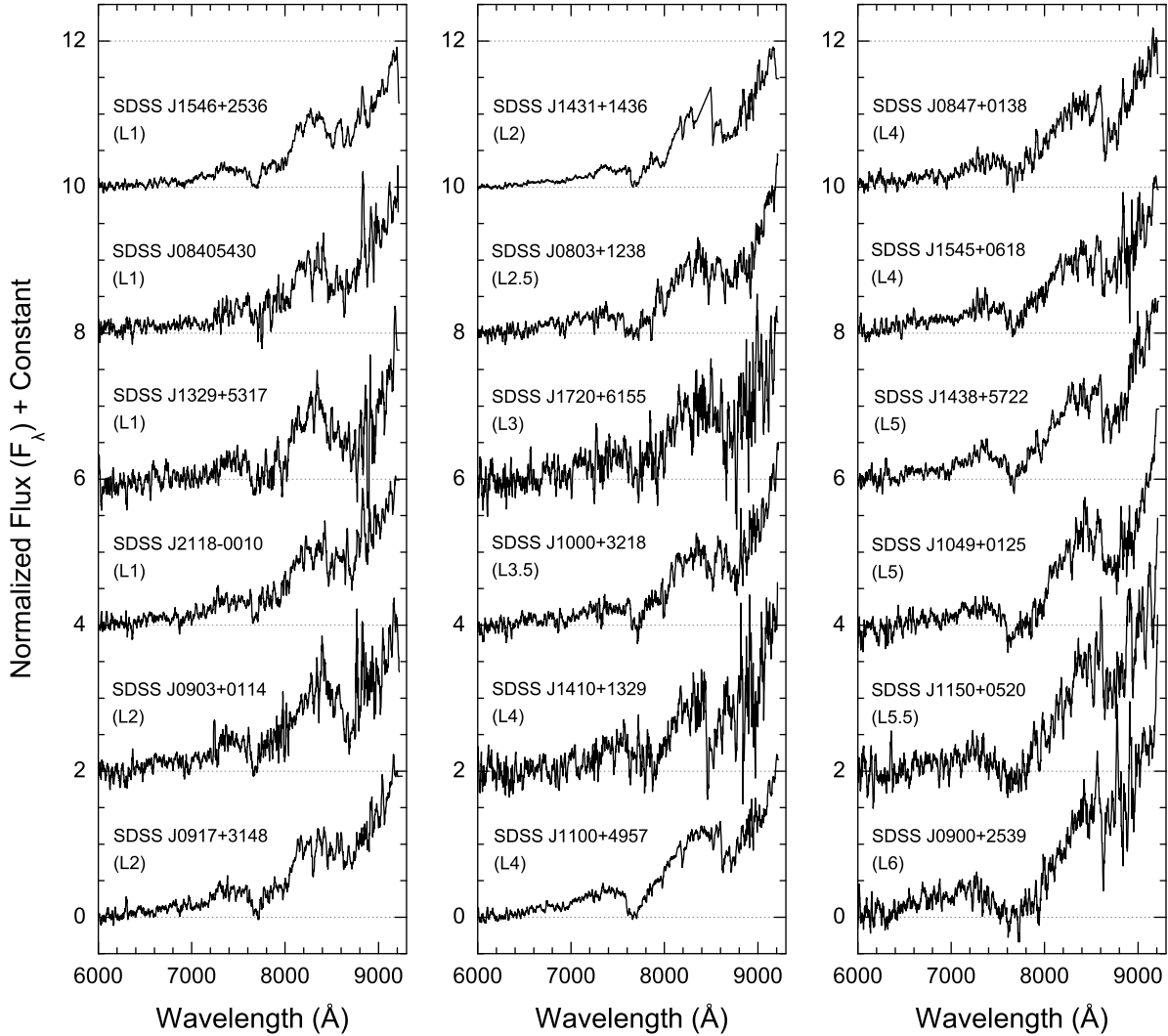


Fig. 5. The SDSS spectra of new M and L dwarfs. Same as Figure 4.

proper motions measured from UKIDSS and SDSS images are given in columns 2 and 3 of Table 6. Database proper motions (i.e. calculated from cross-database coordinate/epoch information) for UKIDSS/SDSS, 2MASS/UKIDSS, and 2MASS/SDSS database combinations are given in columns 4-9 of Table 6, and for the UKIDSS/SDSS combination in columns 6-7 of Table 3. A correction for systematic coordinate uncertainties between UKIDSS and 2MASS/SDSS was decreased as before (see section 3). Figure 8 shows average proper motions of reference objects of objects in Table 6 which proper motions measured with 2MASS-SDSS-UKIDSS databases. The proper motion offsets of 2MASS-UKIDSS with the longest baseline have the smallest offsets ($<0.008''\text{yr}^{-1}$) which indicated proper motion with a baseline of longer than 5 years (e.g. 2MASS-UKIDSS) will be a very good way for identified ultracool dwarfs.

- In most cases the 2MASS-SDSS proper motions calculated from the databases are in reasonable agreement with

our derived relative proper motions to within the uncertainties. However, the uncertainties associated with the relative proper motions are often larger. This is because in general there is a reduced number of useful reference sources in the 2MASS images. This can sometimes be compounded if a sources is close to the edge of a 2MASS strip, since the number of reference sources can be reduced still further. We thus conclude that the database proper motions are to be preferred when combining 2MASS and SDSS survey data.

- In general, the UKIDSS/SDSS, 2MASS/UKIDSS and 2MASS/SDSS database proper motions agree well to within their uncertainties, except in a limited number of cases, where we find that on closer inspection the baseline between the database epochs is low and the 2MASS sources themselves are near the 2MASS detection limit. The 2MASS/SDSS database proper motions thus stand up reasonably well when compared to those measured from a combination of, on average, higher signal-to-noise imaging data.

Table 4. Parameters of fitting equations for color–type relationships.

Color	a	b	c	Type Range	R	Sensitivity Index ^a
r–i	2.77242	0.01930	–0.00355	[10,27.5]	0.62	0.073
i–z	0.89637	0.00812	0.00582	[13,25]	0.89	0.225
i–J	4.46097	–0.12872	0.01099	[10,25]	0.94	0.253
i–H	2.68743	0.22692	0	[10,25]	0.92	0.227
i–K	2.04847	0.39856	–0.00567	[10,25]	0.90	0.200
z–J	1.32530	0.10725	0	[10,13.5]	0.59	0.107
z–J	0.61620	0.10826	0	[19,26]	0.81	0.107
z–H	4.23705	–0.31004	0.02038	[10,14]	0.70	0.158
z–H	4.60067	–0.03962	0	[17.5,27.5]	0.53	0.040
z–K	3.93079	–0.21325	0.01860	[10,14]	0.72	0.235
z–K	6.96601	–0.13083	0	[17.5,27.5]	0.72	0.080
H–K	0.15050	0.03638	0	[10,15]	0.40	0.040
H–K	2.19557	–0.08809	0	[17,25]	0.66	0.088
J–H	0.06224	0.06903	0	[10,14]	0.49	0.088
J–H	5.58544	–0.21707	0	[20,25]	0.90	0.100

Notes: The united polynomial fitting equation of color–spectral type relationships is: $color = a + b(type) + c(type)^2$, type=10 for L0, 15 for L5, 20 for T0, 25 for T5.

^a Sensitivity indices are the rates of change of color ranges with spectral ranges covered by fitting lines.

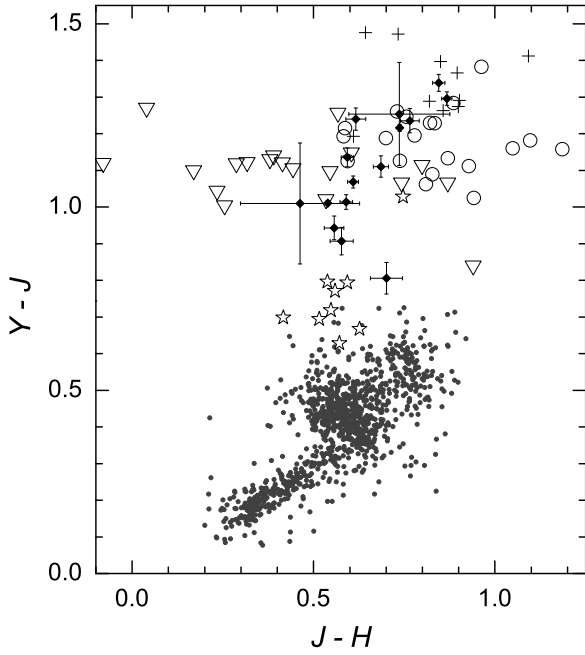


Fig. 7. $Y-J$ vs. $J-H$ diagram for known M, L and T dwarfs and 15 ultracool dwarf candidates (diamonds) which have Y band photometric data from UKIDSS, include 4 objects with SDSS spectra. M5.5-M8.5 (open pentacles), L0-L4.5 (crosses), L5-L9.5 (open circles), T0-T3.5 (open triangles) and 1024 sources from UKIDSS LAS in 1 deg^2 with $Y < 18.5$ (gray points). The J band photometric data of the two with the very large errors used here are transformed from 2MASS.

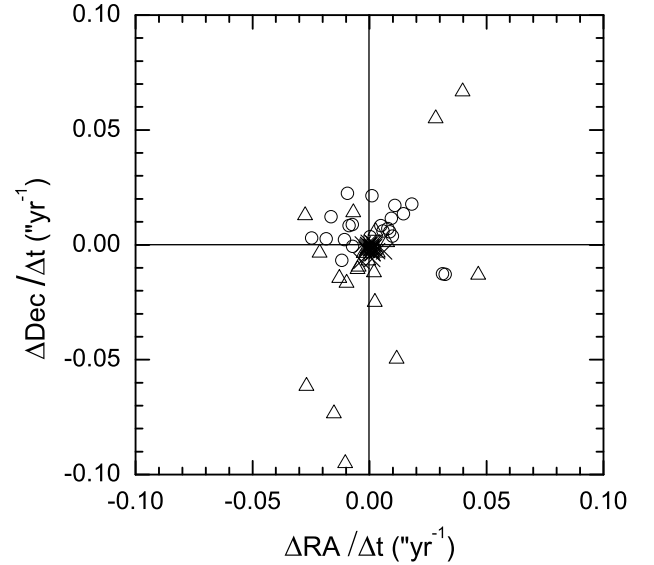


Fig. 8. Average proper motions of reference objects for ultra-cool dwarf candidates in Table 6. Different symbols indicated systematic corrections used for different survey combinations, 2MASS-SDSS (open triangles, 21 objects), SDSS-UKIDSS (open circles, 23 objects) and 2MASS-UKIDSS (crosses, 23 objects).

mated uncertainties from each method are comparable. This result is not surprising, but provides a useful verification for our database proper motion calculations.

We thus conclude that overall, our 2MASS-SDSS proper motions calculated from the databases offer a good balance of reasonably accurate measurements over a relatively large sky area.

- The UKIDSS-SDSS proper motions calculated from the databases are in very good agreement with our derived relative proper motions to within the uncertainties, and the esti-

Table 5. Different colors by different spectral types.

Sp.Type	$r-i$	$i-z$	$i-J$	$i-H$	$i-K$	$z-J^a$	$z-H^a$	$z-K^a$	$J-H^a$	$H-K^a$
L0	2.61±0.27	...	4.27±0.17	4.96±0.22	5.47±0.26	2.40±0.13	3.17±0.17	3.66±0.22	0.75±0.11	0.51±0.10
L0.5	2.58±0.35	...	4.32±0.09	5.07±0.05	5.61±0.10	2.45±0.13	3.23±0.09	3.74±0.21	0.79±0.09	0.53±0.07
L1	2.56±0.19	...	4.37±0.12	5.18±0.20	5.75±0.21	2.51±0.12	3.29±0.22	3.84±0.23	0.82±0.14	0.55±0.12
L1.5	2.52±0.10	...	4.43±0.14	5.30±0.27	5.88±0.13	2.56±0.06	3.37±0.13	3.94±0.13	0.86±0.14	0.57±0.09
L2	2.49±0.28	...	4.50±0.23	5.41±0.30	6.01±0.38	2.61±0.21	3.45±0.29	4.05±0.39	0.89±0.18	0.59±0.14
L2.5	2.46±0.33	...	4.57±0.31	5.52±0.23	6.14±0.29	2.67±0.14	3.55±0.16	4.17±0.23	0.93±0.14	0.61±0.13
L3	2.42±0.32	1.99±0.21	4.64±0.36	5.64±0.32	6.27±0.43	2.72±0.19	3.65±0.26	4.30±0.33	0.96±0.17	0.62±0.17
L3.5	2.39±0.64	2.07±0.30	4.73±0.47	5.75±0.53	6.40±0.57	2.77±0.38	3.77±0.48	4.44±0.48	0.99±0.23	0.64±0.24
L4	2.35±0.56	2.15±0.19	4.81±0.33	5.86±0.40	6.52±0.55	...	3.89±0.30	4.59±0.46	1.03±0.28	0.66±0.17
L4.5	2.31±0.55	2.24±0.35	4.91±0.37	5.98±0.21	6.64±0.30	0.68±0.21
L5	2.26±0.53	2.33±0.22	5.00±0.14	6.09±0.27	6.75±0.32	0.70±0.13
L5.5	2.22±0.38	2.42±0.07	5.11±0.27	6.20±0.37	6.86±0.45
L6	2.17±0.75	2.52±0.34	5.21±0.35	6.32±0.51	6.97±0.51
L6.5	2.12±0.55	2.61±0.24	5.33±0.39	6.43±0.43	7.08±0.38
L7	2.07±0.54	2.72±0.44	5.45±0.40	6.55±0.42	7.19±0.48	0.70±0.27
L7.5	2.02±0.93	2.82±0.29	5.57±0.54	6.66±0.53	7.29±0.55	...	3.91±0.42	4.68±0.53	...	0.65±0.18
L8	1.97±0.63	2.93±0.37	5.70±0.35	6.77±0.45	7.39±0.58	...	3.89±0.17	4.61±0.21	...	0.61±0.13
L8.5 ^b	1.91 ...	3.04 ...	5.84 ...	6.89 ...	7.48	3.87 ...	4.55	0.57 ...
L9 ^b	1.86 ...	3.15 ...	5.98±0.75	7.00±0.53	7.57±0.49	2.67±0.27	3.85±0.28	4.48±0.27	...	0.52±0.15
L9.5	1.80±1.38	3.27±0.62	6.13±0.99	7.11±1.15	7.66±1.10	2.73±0.18	3.83±0.34	4.41±0.24	...	0.48±0.20
T0	1.74±1.49	3.39±0.71	6.28±0.42	7.23±0.28	7.75±0.31	2.78±0.29	3.81±0.22	4.35±0.15	1.24±0.23	0.43±0.14
T0.5	1.68±0.65	3.51±0.39	6.44±0.57	7.34±0.44	7.84±0.53	2.84±0.37	3.79±0.25	4.28±0.55	1.14±0.37	0.39±0.45
T1	1.61±0.65	3.63±0.80	6.60±1.09	7.45±0.84	7.92±0.71	2.89±0.30	3.77±0.10	4.22±0.08	1.03±0.09	0.35±0.20
T1.5	1.55±0.42	3.76±0.85	6.77±0.92	7.57±0.88	8.00±0.72	2.94±0.31	3.75±0.31	4.15±0.66	0.92±0.13	0.30±0.24
T2	1.48±1.02	3.89±0.64	6.95±0.68	7.68±0.79	8.07±0.71	3.00±0.10	3.73±0.28	4.09±0.33	0.81±0.17	0.26±0.53
T2.5 ^b	1.41±0.83	4.03±0.85	7.13 ...	7.79 ...	8.15 ...	3.05 ...	3.71 ...	4.02 ...	0.70 ...	0.21 ...
T3	1.34±2.19	4.16±1.58	7.31±1.51	7.91±1.25	8.22±1.19	3.11±0.22	3.69±0.36	3.96±0.50	0.59±0.25	0.17±0.16
T3.5 ^b	1.27 ...	4.30 ...	7.51 ...	8.02 ...	8.28 ...	3.16 ...	3.67 ...	3.89 ...	0.48 ...	0.13 ...
T4 ^b	1.19 ...	4.44 ...	7.70 ...	8.13 ...	8.35 ...	3.21 ...	3.65 ...	3.83 ...	0.38 ...	0.08 ...
T4.5	1.11±1.24	4.59±0.85	7.90±1.02	8.25±0.93	8.41±1.11	3.27±0.11	3.63±0.26	3.76±0.81	0.27±0.20	0.04±0.51
T5	1.04±0.83	4.74±0.62	8.11±0.57	8.36±0.60	8.47±0.79	3.32±0.21	3.61±0.10	3.70±0.40	0.16±0.19	-0.01±0.27
T5.5	0.96±1.45	3.38±0.04	3.59±0.16	3.63±0.73
T6	0.87±1.79	3.43±0.26	3.57±0.36	3.56±0.83
T6.5 ^b	0.79	3.55±0.20	3.50±0.50
T7	0.71±0.77	3.53 ^c ...	3.43 ^c
T7.5 ^b	0.62	3.51 ...	3.37

Notes: Colors of different spectral types are calculated with our fitting equation (equation 9). Standard errors are used.

^a For these colors, the spectral type-color relationships can be double valued. One can rely on indications from the other colors ($i-J$, $i-H$ or $i-z$) to identify the correct value to use.

^b There is only one object available for colors of these subtypes without errors, we prefer to use 0.5 as their errors.

^c No object with this type has data of these colors.

Table 6. Proper motions constraints of SDSS L dwarfs that were also found in UKIDSS DR4.

SDSS Name	Proper Motion ^a ("yr ⁻¹)	Proper Motion Angle ^a	Proper Motion ^b ("yr ⁻¹)	Proper Motion Angle ^c	Proper Motion ^c ("yr ⁻¹)	Proper Motion Angle ^c	Proper Motion ^d ("yr ⁻¹)	Proper Motion Angle ^e
SDSS J004759.59+135332.0	... ^h	...	0.13±0.02	208±10	0.13±0.03	234±14	0.47±0.27	300±36
SDSS J015141.04-005156.5	0.044±0.012	274.8±14.2	0.07±0.06	285±57	0.04±0.03	257±72	0.07±0.15	150 ...
SDSS J022927.95-005328.5	0.068±0.012	104.8±25.1	0.02±0.03	57 ...	0.04±0.04	136 ...	0.10±0.09	143±63
SDSS J073241.77+264558.9	0.002 ...	30.3 ...	0.04±0.02	359±32	0.02±0.03	230 ...	0.12±0.06	206±30
SDSS J074436.02+251330.5	0.033 ...	262.6 ...	0.04±0.03	296±50	0.06±0.06	296 ...	0.05±0.28	322 ...
SDSS J075754.16+221604.9	0.016 ...	74.6 ...	0.02±0.04	63 ...	0.05±0.04	116±59	0.11±0.07	124±38
SDSS J081303.96+243355.9	0.066 ...	251.3 ...	0.06±0.03	254±30	0.08±0.03	228±25	0.09±0.06	216±42
SDSS J081409.45+260250.4	0.057 ...	278.5 ...	0.06±0.03	304±35	0.03±0.03	217±59	0.08±0.05	170±36
SDSS J083613.45+022106.2	0.096±0.003	285.0±1.6	0.07±0.02	311±17	0.11±0.03	291±14	0.36±0.16	263±26
SDSS J092745.81+010640.4	0.100±0.001	274.1±2.0	0.12±0.02	272± 9	0.10±0.03	302±19	... ^g	37±58
SDSS J094624.37+344639.8	0.083 ...	293.8 ...	0.09±0.03	304±22	0.07±0.04	298±33	0.05±0.07	295 ...
SDSS J095941.47+114146.0	0.148 ...	254.1 ...	0.15±0.03	259±12	0.14±0.04	257±18	0.11±0.10	252±67
SDSS J121238.73+000721.6	0.037 ...	278.5 ...	0.03±0.02	342±38	0.04±0.05	282 ...	0.13±0.27 ^f	20 ...
SDSS J133131.70+122531.4	0.182±0.006	193.7±1.4	0.16±0.03	188±11	0.12±0.02	207± 8	0.12±0.03	243±14
SDSS J134531.43+001551.2	0.047±0.006	95.2±1.9	0.05±0.02	77±22	0.04±0.05	124 ...	0.25±0.27 ^f	34 ...
SDSS J150153.00-013507.1	0.236±0.002	255.3±0.7	0.26±0.03	264± 6	0.24±0.02	258± 5	0.21±0.07	241±19
SDSS J154236.26-004545.9	0.531±0.001	258.5±0.1	0.52±0.02	259± 2	0.60±0.05	252± 5	... ^g	40±25
SDSS J154432.77+265551.2	0.141 ...	311.9 ...	0.16±0.04	310±15	0.15±0.03	304±11	0.18±0.05	295±16
SDSS J154740.16+053208.3	0.047±0.006	293.1±3.9	0.06±0.05	327±46	0.06±0.05	243±54	0.16±0.11	209±43
SDSS J161711.68+322249.5	0.099 ...	213.0 ...	0.04±0.04	61 ...	0.02±0.04	107 ...	0.02±0.06	173 ...
SDSS J232715.71+151730.4	0.160±0.001	202.4±0.7	0.20±0.02	216± 5	0.18±0.02	211± 5	0.10±0.04	210±28
SDSS J234040.33-003337.2	0.028±0.003	258.8±6.4	0.05±0.04	49±57	0.01±0.04	199 ...	0.05±0.08	214 ...
SDSS J234513.85+002441.6	0.092±0.001	200.1±4.2	0.29±0.03	189± 7	0.05±0.05	221 ...	1.04±0.26	4±14

- ^a SDSS-UKIDSS relative proper motions - found by specifically measuring the relative movement of the ultracool dwarfs with respect to nearby reference objects in the SDSS and UKIDSS images.
- ^b SDSS-UKIDSS data-base proper motions - found by dividing the difference between the SDSS and UKIDSS coordinates (from the respective databases) by the observational epoch difference. Standard errors are calculated using the major axes of the position error ellipses from SDSS and UKIDSS.
- ^c 2MASS-UKIDSS database proper motions - as for *b* except using 2MASS and UKIDSS.
- ^d 2MASS-SDSS database proper motions - as for *b* except using 2MASS and SDSS. We do not present the proper motions calculated with a baseline 10 months.
- ^e Error ellipses of 2MASS and SDSS overlap for some objects for which position angle errors are not meaningful.
- ^f Objects with a 2MASS-SDSS baseline < 1 year.
- ^g We do not present their proper motions for they have a short 2MASS-SDSS baseline (< 2 months).
- ^h We do not measure its proper motion for it is very faint in SDSS *z*-band image.

6. Discussion

Although our photometric selection criteria have been shown to be optimized for mid-late L dwarfs (see Figure 1), most of the sample that had SDSS spectra are actually late M and early L dwarfs. This partly results from a luminosity bias since later, less luminous L dwarfs are only detected by SDSS in a smaller volume. SDSS targeting priority for these objects was primarily determined through brightness, so our spectroscopic sample is reasonably close to a magnitude limited subset of our full photometric selection. However, in addition, later L dwarfs are redder, and are more likely to become *i*-band drop outs, precluding their selection in our sample. For our full sample, we reach fainter magnitudes and thus identify more later L dwarfs. The spectral type distribution of the candidates without spectra (i.e. based on the relationship between spectral type and colors) spans a range out to T3, with many candidates in the L0-L7 range.

Our spectral typing procedure makes use of numerous optical, near infrared and optical-infrared colors. Overall we find that the $i-z$, $i-J$, $i-H$ and $i-K$ colors are the most useful. For the objects in Table 1, the spectral types based on SDSS spectra and those based on colors generally agree with each other well. However, we caution against the use of $i-z$ for estimating spectral types earlier than L3, as Figure 3 shows $i-z$ does not correlate well in this range. In our analysis, if the $i-J$ and $i-H$ colors indicate a spectral type earlier than L3, then we do not include an estimated type based on the $i-z$ color. The addition of UKIDSS photometry adds an additional means to constrain spectral type (e.g. using $Y-J$), particularly in and around the L-T transition (\sim L7-T3). With the increasing coverage of UKIDSS we can refine our selection techniques through additional color-spectral type relationships in the near future.

Of the 36 objects with SDSS spectra, 19 have 2σ detections of non-zero proper motions from SDSS-2MASS, 10 of which have proper motions above $0.2''\text{yr}^{-1}$ (see, Table 1). There are fewer 2σ proper motion detections for objects without spectra because they are, on average, further away. For SDSS-2MASS match, a matching radius of $6''$ might lead to the loss of a small number high proper motion objects (e.g. proper motion larger than $1''\text{yr}^{-1}$ and baseline longer than 6 years). Some objects in Table 1, 6 and 7 (online data) have larger proper motions (also with large errors) but usually have a shorter baseline (even less than a year) and these proper motions are not very reliable. The errors in our proper motion measurements are dominated by 2MASS positional uncertainties (especially for objects with shorter baselines), however we have shown through a variety of comparisons that our 2MASS-SDSS database proper motions are of reasonable quality and can thus provide an additional tool to identify large samples of L dwarfs in the SDSS sky. In the future, a SDSS second epoch and surveys such as Pan-STARRS will offer an even more powerful means to efficiently select late M and L dwarfs through their proper motion.

It is clear that SDSS combined with 2MASS and now UKIDSS, offers a powerful means to select large populations of L dwarfs using spectroscopy, photometry and astrometry. As the sample of known L dwarfs grows we can expect to reveal a broader range of inherent properties (e.g. composition, mass, age, kinematics). Higher signal-to-noise and resolution spectroscopic observations could be used to study such interesting sub-populations e.g. by searching for the presence of lithium to directly assess age and mass (Pavlenko et al. 2007) and the use of higher resolution cross correlation techniques to measure radial velocities and space motions, yielding important kinematic information.

Acknowledgements. Funding for the SDSS and SDSS-II has been provided by the Alfred P. Sloan Foundation, the Participating Institutions, the National Science Foundation, the U.S. Department of Energy, the National Aeronautics and Space Administration, the Japanese Monbukagakusho, the Max Planck Society, and the Higher Education Funding Council for England. The SDSS Web Site is <http://www.sdss.org/>.

The SDSS is managed by the Astrophysical Research Consortium for the Participating Institutions. The Participating Institutions are the American Museum of Natural History, Astrophysical Institute Potsdam, University of Basel, University of Cambridge, Case Western Reserve University, University of Chicago, Drexel University, Fermilab, the Institute for Advanced Study, the Japan Participation Group, Johns Hopkins University, the Joint Institute for Nuclear Astrophysics, the Kavli Institute for Particle Astrophysics and Cosmology, the Korean Scientist Group, the Chinese Academy of Sciences (LAMOST), Los Alamos National Laboratory, the Max-Planck-Institute for Astronomy (MPIA), the Max-Planck-Institute for Astrophysics (MPA), New Mexico State University, Ohio State University, University of Pittsburgh, University of Portsmouth, Princeton University, the United States Naval Observatory, and the University of Washington.

This work is based in part on data obtained as part of the UKIRT Infrared Deep Sky Survey. This publication makes use of data products from the Two Micron All Sky Survey. This research has made use of the VizieR catalogue access tool, CDS, Strasbourg, France. Research has benefitted from the M, L, and T dwarf compendium housed at DwarfArchives.org and maintained by Chris Gelino, Davy Kirkpatrick, and Adam Burgasser. This work was part supported by the Natural Science Foundation of China under Grant Nos 10521001, 10433030, 10503010 and the CAS Research Fellowship for International Young Researchers.

References

- Adelman-McCarthy, J., K., Aguiros, M. A., Allam, S. S., et al. 2007, *ApJS*, 172, 634
- Adelman-McCarthy, J., K., Aguiros, M. A., Allam, S. S., et al. 2008, *ApJS*, 175, 297
- Baraffe, I., Chabrier, G., Baraman, T. s., et al. 2003, *A&A*, 402, 701
- Becklin, E. E., & Zuckerman, B. 1988, *Nature*, 336, 656
- Bessell, M. S. 1991, *AJ*, 101, 662
- Bochanski, J. J., West, A. A., Hawley, S. L. & Covey, K. R. 2007, *AJ*, 133, 531
- Burgasser, A. J., Kirkpatrick, J. D., Brown, M. E., et al. 1999, *ApJ*, 522, L65
- Burgasser, A. J., Kirkpatrick, J. D., Brown, M. E., et al. 2002, *ApJ*, 564, 421
- Burgasser, A. J., McElwain, M. W., Kirkpatrick, J. D., et al. 2004, *AJ*, 127, 2856
- Burningham, B., Pinfield, D. J., Leggett, S. K., et al. 2008, *MNRAS*, acpted
- Chiu, K., Fan, X., Leggett, S. K., et al. 2006, *AJ*, 131, 2722
- Cruz, K. L., Reid, I. N., Liebert, J., Kirkpatrick, J. D. & Lowrance, P. J. 2003, *AJ*, 126, 2421
- Cruz, K. L., Reid, I. N., Kirkpatrick, J. D., et al. 2007, *AJ*, 133, 439
- Delfosse, X., Tinney, C. G., Forveille, T., et al. 1997, *A&A*, 327, L25
- Epchtein, N., de Batz, B., Capolani, L., et al. 1997, *The ESO Messenger*, 87, 27
- Fan, X., Knapp, G. R., Strauss, M. A., et al. 2000, *AJ*, 119, 928
- Geballe, T. R., Knapp, G. R., Leggett, S. K., et al. 2002, *ApJ*, 564, 466
- Gizis, J. E., Monet, D. G., Reid, et al. 2000, *AJ*, 120, 1085
- Hawley, S. L., Covey, K. R., Knapp, G. R., et al. 2002, *AJ*, 123, 3409
- Hewett, P. C., Warren, S. J., Leggett, S. K. & Hodgkin, S. T. 2006, *MNRAS*, 367, 454
- Kendall, T. R., Maun, N., Azzopardi, M., et al. 2003, *A&A*, 403, 929
- Kendall, T. R., Jones, H. R. A., Pinfield, D. J., et al. 2007a, *MNRAS*, 374, 445
- Kendall, T. R., Tamura, M., Tinney, C. G., et al. 2007b, *A&A*, 466, 1059
- Kirkpatrick, J. D., Reid, I. N., Liebert, J., et al. 1999, *ApJ*, 519, 802
- Kirkpatrick, J. D., Reid, I. N., Liebert, J., et al. 2000, *AJ*, 120, 447
- Knapp, G. R., Leggett, S. K., Fan, X., et al. 2004, *AJ*, 127, 3553
- Lawrence, A., Warren, S. J., Almaini, O., et al. 2007, *MNRAS*, 379, 1599
- Lodieu, N., Pinfield, D. J., Leggett, S. K., et al. 2007, *MNRAS*, 379, 1423
- Looper, D. L., Kirkpatrick, J. D. & Burgasser, A. J. 2007, *AJ*, 134, 1162
- Nakajima, T., Oppenheimer, B. R., Kulkarni, S. R., et al. 1995, *Nature*, 378, 463
- Pavlenko, Ya. V., Jones, H. R. A., Martin, E. L., et al. 2007, *MNRAS*, 380, 1285
- Pinfield, D. J., Burningham, B., Tamura, M., et al. 2008, *MNRAS*, 390, 304
- Reid, I. N., Cruz, K. L., Kirkpatrick, J. D., et al. 2008, *AJ*, 136, 1290
- Schneider, D. P., Knapp, G. R., Hawley, S. L., et al. 2002, *AJ*, 123, 458
- Schmidt, S. J., Cruz, K. L., Bongiorno, B. J., Liebert, J. & Reid, I. N. 2007, *AJ*, 133, 2258
- Skrutskie, M. F., Cutri, R. M., Stiening, R., et al. 2006, *AJ*, 131, 1163
- Stoughton, C., Lupton, R. H., Bernardi, M., et al. 2002, *AJ*, 123, 485
- Warren, S. J., Mortlock, D. J., Leggett, S. K., et al. 2007, *MNRAS*, 381, 1400
- York, D. G., Adelman, J., Anderson, J. E., Jr., et al. 2000, *AJ*, 120, 1579

Online Material

Table 7. SDSS and 2MASS photometry of 129 ultra-cool dwarf candidates

SDSS Name	SDSS r	SDSS i	SDSS z	2MASS J	2MASS H	2MASS K	Proper Motion ("yr ⁻¹)	Proper Motion Angle	Sp. Type by Colors
SDSS J073813.07+155304.7	23.76±0.42	21.26±0.08	19.25±0.06	16.89±0.20	16.07±0.21	15.37±0.17	0.04±0.04	184 ...	L1
SDSS J074151.17+275837.6	23.60±0.56	21.51±0.15	19.39±0.07	17.31±0.18	16.67±0.21	15.95±0.23	0.05±0.08	315 ...	L0
SDSS J074838.61+174332.9	23.89±0.46	21.35±0.07	19.06±0.05	16.27±0.11	15.18±0.09	14.42±0.09	0.07±0.02	264±14	L7
SDSS J075635.25+363033.6	22.26±0.20	19.85±0.06	17.07±0.01	15.24±0.04	14.61±0.05	14.09±0.05	0.11±0.11	149 ...	L2.5
SDSS J075752.70+091410.0	22.86±0.27	20.62±0.05	18.57±0.03	15.86±0.08	14.83±0.07	14.09±0.06	0.14±0.02	249± 8	L4
SDSS J075923.05+462007.4	24.18±0.66	21.44±0.12	19.30±0.06	17.00±0.16	16.09±0.13	15.86±0.23	0.23±0.25	297 ...	L2
SDSS J080020.39+360627.1	23.61±0.43	21.24±0.08	19.23±0.06	16.64±0.13	15.93±0.16	15.62±0.19	0.37±0.25	141±42	L2.5
SDSS J080138.61+372205.8	23.00±0.23	20.59±0.08	18.21±0.02	16.83±0.22	15.84±0.22	15.45±0.19	0.22±0.13	254±35	...
SDSS J080252.73+051058.3	23.59±0.64	20.72±0.09	18.67±0.06	16.16±0.11	15.30±0.09	14.91±0.14	0.06±0.04	270±44	L2
SDSS J081215.88+504758.3	23.15±0.32	20.71±0.05	18.69±0.04	16.37±0.13	15.70±0.18	15.28±0.17	0.24±0.05	232±12	L0.5
SDSS J081409.11+281909.6	24.25±0.74	21.69±0.18	19.58±0.10	17.45±0.23	16.47±0.21	15.79±0.18	0.17±0.07	246±23	L0.5
SDSS J081825.78+374103.1	23.32±0.27	21.70±0.10	19.43±0.06	16.94±0.20	16.01±0.19	15.44±0.18	0.19±0.10	65±32	L3.5
SDSS J081843.64+175645.7	23.14±0.34	21.61±0.15	19.44±0.09	17.01±0.19	16.02±0.19	15.45±0.17	0.07±0.05	349±47	L2.5
SDSS J081905.47+493118.5	23.75±0.54	21.23±0.09	19.19±0.06	17.09±0.23	16.51±0.31	15.56±0.21	L0
SDSS J081951.43+543155.1	23.71±0.50	21.02±0.08	18.97±0.06	16.97±0.19	15.91±0.14	15.45±0.20	0.13±0.06	179±30	L1
SDSS J082059.29+280648.0	23.22±0.36	21.22±0.09	19.12±0.06	16.92±0.21	15.89±0.19	15.40±0.16	0.08±0.10	240 ...	L1
SDSS J082213.75+510120.2	23.46±0.43	20.85±0.07	18.81±0.05	16.57±0.12	15.66±0.12	15.17±0.12	L0.5
SDSS J083301.44+445107.6	23.45±0.43	21.19±0.08	19.12±0.05	16.54±0.14	15.96±0.19	15.42±0.20	0.56±0.22	152±23	L2
SDSS J084537.80+293137.2	23.74±0.42	21.47±0.11	19.42±0.06	16.74±0.12	15.97±0.13	15.14±0.12	0.07±0.04	124±33	L2.5
SDSS J084737.45+462443.8	23.16±0.50	20.92±0.09	18.87±0.07	16.88±0.17	16.03±0.19	15.78±0.23	0.02±0.17	76
SDSS J084750.21+510846.3	23.08±0.44	20.83±0.08	18.79±0.04	16.66±0.14	16.00±0.15	15.24±0.15	0.20±0.20	312±83	L0
SDSS J084838.93+484025.4	23.07±0.27	21.04±0.07	19.03±0.05	16.59±0.13	15.77±0.13	15.29±0.15	0.55±0.10	106±11	L2
SDSS J085048.96+173210.9	23.33±0.30	20.89±0.06	18.88±0.05	16.57±0.12	15.93±0.15	15.23±0.11	0.15±0.03	354±12	L0.5
SDSS J085117.58+583226.6	24.25±0.76	21.59±0.13	19.53±0.09	17.07±0.19	16.45±0.23	15.84±0.23	0.03±0.07	257 ...	L1.5
SDSS J085119.69+104348.0	24.36±0.65	21.79±0.11	19.58±0.05	16.79±0.15	15.78±0.15	15.09±0.12	0.23±0.03	309± 7	L5
SDSS J085711.43+415928.6	23.72±0.53	21.46±0.11	19.39±0.07	17.37±0.24	16.18±0.20	15.73±0.22	0.26±0.10	129±21	L2
SDSS J090308.17+165935.5	24.87±0.59	21.61±0.10	19.38±0.07	16.49±0.11	15.78±0.16	15.49±0.19	0.11±0.04	129±20	L6
SDSS J090435.90+322918.7	23.71±0.52	21.05±0.07	19.02±0.05	16.97±0.17	16.22±0.20	15.45±0.20	0.38±0.06	294±10	...
SDSS J090546.54+562311.9	23.01±0.36	20.28±0.05	18.24±0.03	15.40±0.05	14.28±0.04	13.73±0.04	L4
SDSS J091428.64+230541.2	24.66±0.72	21.26±0.08	19.14±0.05	16.62±0.10	15.53±0.08	14.90±0.08	0.05±0.02	311±22	L3
SDSS J091811.89+390216.7	23.77±0.62	22.07±0.21	19.65±0.10	17.02±0.21	16.15±0.21	15.57±0.22	0.07±0.10	234 ...	L5.5
SDSS J091816.02+481300.4	23.02±0.23	20.75±0.05	18.74±0.05	16.43±0.12	15.52±0.12	15.30±0.14	0.14±0.06	71±27	L0.5
SDSS J092752.44+572932.5	23.90±0.51	21.37±0.09	19.36±0.07	16.65±0.15	15.46±0.13	14.84±0.11	L3.5
SDSS J092819.74+180510.8	23.64±0.35	22.20±0.15	19.98±0.08	17.23±0.21	16.65±0.26	15.90±0.21	0.25±0.05	289±11	L3.5
SDSS J093100.69+605539.6	23.64±0.58	21.10±0.10	19.00±0.07	16.48±0.11	15.69±0.10	15.30±0.13	0.44±0.15	280±20	L2.5
SDSS J093204.02+345937.0	25.18±0.73	21.97±0.22	19.92±0.10	17.01±0.18	16.22±0.19	15.46±0.21	0.23±0.07	149±16	L4.5
SDSS J093956.05+242658.7	24.85±0.64	22.07±0.23	19.69±0.10	16.97±0.22	15.93±0.22	15.53±0.21	0.36±0.05	244± 8	L6.5
SDSS J094146.38+215843.5	25.07±0.58	21.78±0.11	19.67±0.09	16.94±0.18	15.92±0.18	15.55±0.17	0.09±0.04	244±26	L4
SDSS J094427.33+641037.3	22.96±0.33	20.95±0.08	18.93±0.06	16.67±0.16	15.88±0.17	15.46±0.18	0.09±0.06	296±38	L0
SDSS J094429.58+465254.7	22.84±0.32	21.26±0.11	19.16±0.06	17.26±0.21	16.58±0.23	16.09±0.25	0.06±0.16	322
SDSS J095154.19+282040.8	23.10±0.30	21.22±0.08	19.21±0.06	16.56±0.16	16.06±0.15	15.52±0.18	0.07±0.05	298±44	L2
SDSS J095932.74+452330.5	23.73±0.51	21.04±0.08	19.01±0.05	15.88±0.07	14.76±0.07	13.67±0.04	0.19±0.05	221±15	L7.5
SDSS J100132.26+492819.9	23.05±0.25	20.74±0.05	18.72±0.04	16.68±0.13	15.95±0.14	15.56±0.18	0.23±0.09	276±23	...

Table 7. continued.

SDSS Name	SDSS r	SDSS i	SDSS z	2MASS J	2MASS H	2MASS K	Proper Motion ("yr ⁻¹)	Proper Motion Angle	Sp. Type by Colors
SDSS J100317.30+331922.0	24.32±0.79	21.60±0.15	19.23±0.07	16.74±0.14	15.73±0.11	15.23±0.14	0.05±0.04	75±56	L4
SDSS J100633.74+363919.5	23.89±0.39	21.60±0.08	19.49±0.05	17.10±0.22	15.98±0.16	15.32±0.19	0.12±0.07	184±32	L2.5
SDSS J101134.72+501400.7	23.79±0.49	21.93±0.15	19.90±0.10	17.60±0.29	16.28±0.20	15.57±0.17	0.70±0.22	259±18	L2
SDSS J101439.66+252511.3	24.45±0.59	21.14±0.07	19.10±0.05	17.24±0.23	16.19±0.21	15.83±0.24	0.09±0.05	215±35	L0
SDSS J101951.13+044944.1	24.10±0.57	21.80±0.15	19.48±0.07	16.85±0.18	16.18±0.20	15.54±0.23	0.57±0.31	240±33	L4
SDSS J102517.57+285113.6	23.64±0.54	20.95±0.07	18.92±0.05	16.54±0.10	15.83±0.12	15.31±0.12	0.11±0.03	288±16	L1.5
SDSS J102546.97+151126.3	24.29±0.70	21.52±0.15	19.47±0.07	16.99±0.15	16.06±0.17	15.42±0.15	0.17±0.04	276±13	L2
SDSS J102935.23+062029.6	24.51±0.55	22.47±0.19	19.37±0.05	16.87±0.22	16.09±0.21	15.02±0.16	0.15±0.14	212±75	L8
SDSS J102939.69+571544.3	24.35±0.52	21.62±0.10	19.17±0.06	16.70±0.13	15.46±0.11	14.99±0.09	0.82±0.07	95±5	L4.5
SDSS J103908.17+244044.1	23.58±0.34	21.73±0.11	19.41±0.06	16.76±0.14	15.72±0.13	15.04±0.11	0.22±0.03	236± 7	L5
SDSS J104808.29+544715.1	23.50±0.40	21.86±0.14	19.46±0.07	16.73±0.19	15.86±0.20	15.43±0.19	0.38±0.11	295±17	L6.5
SDSS J104814.75+135833.3	23.78±0.44	21.94±0.15	19.43±0.07	16.90±0.13	16.01±0.14	15.34±0.14	0.17±0.04	197±14	L5.5
SDSS J105204.75+172241.2	23.14±0.34	21.27±0.10	19.21±0.06	16.71±0.11	16.04±0.14	15.53±0.16	0.31±0.03	158± 6	L1.5
SDSS J105254.02+584951.2	23.96±0.37	21.44±0.08	19.26±0.04	16.44±0.12	15.44±0.13	14.87±0.10	0.09±0.05	54±37	L5
SDSS J110827.31+083801.8	23.74±0.71	22.39±0.34	19.26±0.07	16.58±0.16	15.50±0.11	15.03±0.16	0.34±0.08	217±14	L8.5
SDSS J111501.36+160701.5	22.94±0.37	20.71±0.07	18.59±0.05	16.40±0.12	15.22±0.09	14.56±0.11	0.34±0.08	248±14	L1
SDSS J111802.89+060703.6	24.09±0.53	21.42±0.10	19.35±0.05	17.00±0.18	16.27±0.21	15.66±0.26	0.28±0.11	133±23	L1.5
SDSS J111910.46+055248.4	23.39±0.33	21.67±0.11	19.60±0.06	16.76±0.16	15.48±0.11	15.03±0.15	0.07±0.16	109 ...	L5
SDSS J112012.95+212520.4	23.50±0.42	21.65±0.11	19.53±0.06	16.90±0.17	15.79±0.14	15.34±0.14	0.13±0.04	198±16	L4
SDSS J112722.94-003714.4	23.53±0.33	21.34±0.08	19.24±0.05	16.81±0.18	16.12±0.26	15.35±0.20	L1.5
SDSS J113022.46+122751.6	23.49±0.48	21.69±0.13	19.64±0.10	17.05±0.18	16.47±0.22	15.98±0.24	0.16±0.11	358±41	L2
SDSS J113639.67+485240.3	23.54±0.31	20.91±0.05	18.86±0.03	16.16±0.10	15.27±0.11	14.58±0.08	0.20±0.06	307±17	L3.5
SDSS J114103.28+632805.9	23.57±0.41	21.50±0.12	19.46±0.07	16.72±0.13	15.94±0.13	15.62±0.23	0.45±0.18	308±23	L3
SDSS J114302.72+190541.9	24.77±0.62	22.76±0.26	19.77±0.08	16.77±0.18	15.80±0.15	15.01±0.14	0.26±0.03	172± 8	L9
SDSS J114807.23+390106.9	24.12±0.66	21.23±0.08	19.19±0.05	16.92±0.18	15.96±0.17	15.52±0.17	0.20±0.06	323±18	L1.5
SDSS J115017.36+512502.4	24.28±0.60	22.02±0.18	19.98±0.11	16.87±0.20	16.03±0.18	15.08±0.12	0.15±0.12	221±51	L6
SDSS J115058.98+440917.2	24.06±0.58	21.38±0.09	19.37±0.06	17.05±0.19	16.15±0.23	15.49±0.15	0.14±0.06	272±26	L1
SDSS J115722.81+264119.6	23.71±0.47	21.06±0.07	18.89±0.04	16.71±0.12	15.91±0.15	15.02±0.11	0.06±0.03	263±25	L1
SDSS J115820.75+043501.7	22.00±0.20	20.36±0.07	17.95±0.04	15.61±0.06	14.68±0.06	14.44±0.06	0.86±0.86	316 ...	L3
SDSS J120136.14+135005.9	22.76±0.17	20.66±0.05	18.63±0.04	16.88±0.13	16.14±0.17	15.74±0.16	0.03±0.04	94
SDSS J120337.00+445333.4	23.85±0.45	21.74±0.12	19.52±0.06	17.43±0.25	16.55±0.25	15.56±0.18	0.24±0.08	281±20	L0.5
SDSS J121846.56+410016.0	24.87±0.71	21.74±0.13	19.61±0.07	16.74±0.16	15.58±0.13	15.13±0.15	0.05±0.05	118 ...	L5.5
SDSS J122218.47+364348.4	22.61±0.17	20.21±0.03	18.15±0.03	15.97±0.08	15.27±0.10	14.85±0.09	0.27±0.04	92± 9	L0
SDSS J122449.44+502154.1	23.98±0.45	21.62±0.10	19.14±0.06	16.53±0.13	15.66±0.11	14.86±0.10	0.48±0.05	204± 6	L6
SDSS J123256.67+484417.0	22.21±0.18	20.54±0.06	18.54±0.03	16.47±0.18	15.59±0.14	15.32±0.20	0.44±0.11	254±15	L0
SDSS J124151.85+561541.6	23.44±0.42	20.86±0.07	18.81±0.04	16.42±0.11	15.61±0.12	14.95±0.11	0.04±0.04	314±77	L2
SDSS J124609.07+294200.1	24.07±0.48	21.30±0.08	19.26±0.05	16.97±0.19	16.12±0.21	15.65±0.24	0.02±0.06	331 ...	L1
SDSS J124655.54+535342.8	23.89±0.47	21.31±0.08	19.24±0.05	16.37±0.11	15.57±0.12	14.98±0.12	0.17±0.09	160±33	L4
SDSS J125002.99+484834.3	23.99±0.47	21.93±0.16	19.88±0.09	17.30±0.26	15.82±0.14	15.25±0.14	0.37±0.15	263±24	L4
SDSS J125137.76+462026.0	22.94±0.21	20.59±0.05	18.50±0.03	15.83±0.08	14.75±0.07	14.48±0.10	0.31±0.02	172± 4	L4
SDSS J125410.69+382546.0	23.80±0.46	21.48±0.11	19.42±0.06	16.88±0.15	16.11±0.18	15.65±0.16	0.06±0.04	239±47	L2.5
SDSS J125438.50+434657.2	23.70±0.48	22.22±0.22	19.47±0.07	16.81±0.15	15.35±0.10	14.81±0.09	0.20±0.04	257±11	L8.5
SDSS J130449.88+010627.0	23.10±0.31	21.37±0.10	19.30±0.06	16.69±0.17	15.80±0.17	15.12±0.17	0.83±0.24	125±17	L3

Table 7. continued.

SDSS Name	SDSS r	SDSS i	SDSS z	2MASS J	2MASS H	2MASS K	Proper Motion ("yr ⁻¹)	Proper Motion Angle	Sp. Type by Colors
SDSS J131142.11+362923.9	23.08±0.23	20.49±0.04	18.31±0.03	15.55±0.05	14.75±0.06	14.14±0.05	0.40±0.02	279± 3	L4
SDSS J131218.20+284643.0	24.13±0.57	21.36±0.09	19.31±0.06	17.27±0.26	16.33±0.32	15.72±0.21	0.10±0.09	219±58	L0
SDSS J132535.68+504007.0	24.45±0.54	21.56±0.08	19.38±0.05	16.93±0.23	15.86±0.23	15.46±0.23	0.32±0.15	288±27	L3
SDSS J133316.06+374421.7	23.31±0.29	21.01±0.06	18.65±0.03	15.89±0.06	14.90±0.05	14.30±0.05	0.12±0.04	76±18	L6.5
SDSS J134210.11+414023.8	23.65±0.35	21.63±0.11	19.56±0.07	16.86±0.13	15.87±0.12	15.47±0.14	0.20±0.04	229±12	L4
SDSS J135640.46+140205.3	23.83±0.35	20.96±0.08	18.36±0.03	16.62±0.15	16.10±0.22	15.28±0.15	0.03±0.06	317 ...	L1
SDSS J140058.03+234923.9	23.67±0.39	21.51±0.09	19.48±0.06	16.73±0.17	16.12±0.23	15.38±0.22	0.06±0.06	261 ...	L3
SDSS J140318.98+243718.0	23.56±0.33	21.55±0.09	19.52±0.07	17.18±0.23	16.06±0.22	15.50±0.22	0.03±0.06	194 ...	L1.5
SDSS J141118.49+294850.4	23.52±0.37	21.07±0.07	18.76±0.04	16.20±0.09	15.43±0.11	15.09±0.11	0.28±0.05	164±10	L3.5
SDSS J141405.84+010710.4	23.40±0.38	21.77±0.15	19.63±0.09	16.74±0.20	15.74±0.19	15.25±0.20	L5.5
SDSS J142110.77+472834.3	23.92±0.39	20.40±0.03	18.33±0.02	16.16±0.09	15.33±0.10	14.98±0.13	0.07±0.03	240±22	L0
SDSS J142404.53+184641.4	24.16±0.50	21.41±0.09	19.34±0.06	17.08±0.19	16.44±0.26	15.50±0.16	0.01±0.07	175 ...	L0.5
SDSS J142527.14+300400.4	23.11±0.25	20.78±0.05	18.72±0.03	16.39±0.12	15.54±0.13	15.03±0.12	0.02±0.04	292 ...	L1.5
SDSS J142612.86+313039.4	23.70±0.42	21.39±0.09	19.29±0.05	16.62±0.16	15.59±0.13	14.72±0.09	0.19±0.04	224±11	L4
SDSS J143412.02+271729.9	23.98±0.62	21.41±0.11	19.29±0.07	17.38±0.24	16.33±0.21	15.70±0.21	0.08±0.07	96±68	L0
SDSS J143636.98+465302.7	23.75±0.38	21.92±0.11	19.92±0.08	16.99±0.16	16.13±0.15	15.81±0.20	0.28±0.07	268±15	L4
SDSS J145052.71+462024.8	23.87±0.45	21.68±0.10	19.67±0.09	16.77±0.15	15.93±0.17	15.26±0.14	0.14±0.07	305±32	L4
SDSS J150651.27+553350.7	22.93±0.32	21.10±0.10	19.10±0.08	16.69±0.12	15.80±0.13	15.30±0.15	0.08±0.11	206 ...	L2
SDSS J151110.91+434036.3	23.48±0.33	21.59±0.09	19.29±0.05	16.60±0.15	15.47±0.13	14.70±0.13	0.24±0.04	152± 9	L5
SDSS J152427.98+024210.1	22.76±0.29	21.21±0.12	19.16±0.06	16.98±0.20	16.39±0.24	15.35±0.17	L0
SDSS J152802.91+013949.6	23.06±0.33	21.38±0.11	19.27±0.12	16.65±0.14	15.75±0.15	15.26±0.17	L3
SDSS J153607.12+203032.6	24.01±0.53	21.81±0.14	19.73±0.10	17.26±0.21	16.17±0.20	15.77±0.24	0.03±0.07	243 ...	L2.5
SDSS J153848.19+360337.5	24.05±0.44	21.68±0.11	19.56±0.05	16.64±0.15	15.76±0.13	15.29±0.14	0.06±0.07	286 ...	L5.5
SDSS J153941.94+531131.0	23.53±0.44	21.44±0.12	19.40±0.07	16.86±0.16	15.95±0.17	15.19±0.18	0.17±0.09	204±34	L2
SDSS J154038.76-001257.1	23.11±0.28	21.60±0.10	19.35±0.06	16.80±0.15	15.67±0.12	15.05±0.14	L4
SDSS J154455.20+330145.1	22.96±0.23	20.54±0.05	18.33±0.02	15.55±0.06	14.52±0.06	13.94±0.05	0.11±0.03	25±15	L5
SDSS J154623.27+333803.2	24.03±0.50	21.13±0.08	19.05±0.05	16.49±0.11	15.77±0.13	15.33±0.14	0.08±0.07	228±54	L2.5
SDSS J155151.04+174216.7	23.34±0.24	21.10±0.06	19.08±0.06	16.70±0.14	15.83±0.15	15.13±0.12	0.12±0.05	320±24	L1.5
SDSS J155702.82+121258.1	23.84±0.55	21.25±0.10	19.19±0.08	17.12±0.25	16.02±0.19	15.51±0.26	0.62±0.05	243± 4	L0.5
SDSS J160022.86+484132.8	23.53±0.44	21.20±0.10	19.06±0.05	16.27±0.09	15.43±0.12	15.01±0.14	0.46±0.09	102±11	L4.5
SDSS J160835.64+120226.8	23.22±0.26	20.56±0.04	18.56±0.03	16.37±0.12	15.35±0.11	15.00±0.14	0.07±0.03	301±28	L0.5
SDSS J160911.45+211658.7	24.02±0.64	21.53±0.14	19.50±0.08	16.96±0.21	15.97±0.20	14.87±0.11	0.09±0.03	30±22	L2
SDSS J161231.01+483357.5	24.34±0.68	21.27±0.08	19.17±0.06	16.20±0.10	15.62±0.12	14.83±0.12	0.11±0.06	320±38	L5.5
SDSS J161459.98+400435.1	22.60±0.19	20.95±0.08	18.93±0.04	16.57±0.12	15.84±0.15	15.01±0.12	0.30±0.04	296± 8	L1
SDSS J161655.06+190842.8	23.57±0.42	21.46±0.09	19.45±0.07	17.18±0.19	16.37±0.22	15.90±0.24	0.06±0.05	305±59	L0
SDSS J163021.84-001801.6	24.80±0.69	22.58±0.24	19.42±0.06	16.25±0.12	15.55±0.15	15.24±0.19	L9.5
SDSS J164939.25+425043.7	24.06±0.46	21.71±0.11	19.48±0.07	16.79±0.14	15.46±0.10	14.79±0.12	0.18±0.05	320±15	L5
SDSS J165914.44+172642.3	24.22±0.48	21.73±0.10	19.69±0.06	16.69±0.16	15.54±0.13	15.15±0.14	0.11±0.06	107±32	L6
SDSS J170418.24+744315.0	23.26±0.30	21.32±0.07	19.07±0.05	16.09±0.09	15.14±0.09	14.27±0.09	0.13±0.04	217±18	L7.5
SDSS J171201.36+324456.6	23.99±0.44	21.29±0.08	19.25±0.07	17.14±0.17	16.26±0.18	15.96±0.24	0.52±0.10	272±11	L0
SDSS J172545.59+640501.2	23.90±0.81	21.90±0.23	19.46±0.09	16.81±0.17	15.89±0.17	15.35±0.20	0.61±0.33	12±33	L6.5
SDSS J172746.49+572247.6	22.53±0.21	20.21±0.04	18.21±0.03	15.83±0.08	14.96±0.09	14.69±0.11	0.14±0.10	33±51	L1.5
SDSS J210515.30-003701.5	24.48±0.60	21.33±0.08	19.10±0.05	16.97±0.17	15.90±0.17	14.91±0.13	0.07±0.07	81±64	L1.5